

MODEL-INDEPENDENT VARIABLE SELECTION VIA THE RULE-BASED VARIABLE PRIORITY

BY MIN LU^{1,a}  AND HEMANT ISHWARAN^{1,b} 

¹*Division of Biostatistics, University of Miami, ^am.lu6@umiami.edu; ^bhishwaran@miami.edu*

While achieving high prediction accuracy is a fundamental goal in machine learning, an equally important task is finding a small number of features with high explanatory power. One popular selection technique is permutation importance, which assesses a variable’s impact by measuring the change in prediction error after permuting the variable. However, this can be problematic due to the need to create artificial data, a problem shared by other methods as well. Another problem is that variable selection methods can be limited by being model-specific. We introduce a new model-independent approach, Variable Priority (VarPro), which works by utilizing rules without the need to generate artificial data or evaluate prediction error. The method is relatively easy to use, requiring only the calculation of sample averages of simple statistics, and can be applied to many data settings, including regression, classification, and survival. We investigate the asymptotic properties of VarPro and show, among other things, that VarPro has a consistent filtering property for noise variables. Empirical studies using synthetic and real-world data show the method achieves a balanced performance and compares favorably to many state-of-the-art procedures currently used for variable selection.

1. Introduction. Although many machine learning procedures are capable of modeling a large number of variables and achieving high prediction accuracy, finding a small number of features with near-equivalent explanatory power is equally desirable. This allows researchers to identify which variables play a prominent role in the problem setting, thus providing insight into the underlying mechanism for what might otherwise be considered a black box. In machine learning, variable selection is often performed using variable importance, described by how much a prediction model’s accuracy depends on the information in each feature [5, 20, 65, 34, 60, 37, 14, 27, 22, 51, 67]. One of the most popular methods is permutation importance, introduced by Leo Breiman in his famous random forests paper [5]. To calculate a variable’s permutation importance, the given variable is randomly permuted in the out-of-sample data (out-of-bag, or OOB, data) and the permuted OOB data is dropped down a tree. OOB prediction error is then calculated. The difference between this and the original OOB error without permutation, averaged over all trees, is the importance of the variable. The larger the permutation importance of a variable, the more predictive the variable.

Because permutation importance is not part of the forest construction and does not make use of the forest ensemble, it can be considered a *filtering (screening)* feature selection method, which refers to selection procedures performed without using a final prediction model. Filtering procedures are widely adopted in many settings, particularly for dealing with ultra-high dimensional data [16, 70, 15, 64, 69]. On the other hand, permutation importance, and other types of prediction-based importance measures, can also be used for *embedded* selection [see, for example, 54], which refers to feature selection processes embedded in the learning phase. An important class of embedded procedures is penalization methods like the

arXiv: 2010.00000

MSC2020 subject classifications: Primary 62GXX; secondary 6208.

Keywords and phrases: Conditional expectation, Released rule, Signal and noise variables, Variable selection.

lasso [63]. Recently, there has been significant attention given to developing variable importance measures that can apply more generally across different types of learning procedures within the framework of model selection [66, 48, 17]. [49] discuss the difference between model selection and variable selection. An example of the latter is the *wrapper* approach [42] for feature subset selection. The term wrapper generally refers to a generic induction algorithm used as a black box to score the feature subsets. Another method worth mentioning is knockoffs [8], which is a screening method that can be applied across different procedures and has the useful property of preserving the false discovery rate.

In this paper, we take a broader approach in the spirit of these latter methods. We call our proposed method VarPro, which refers to a model-independent framework of variable priority. The term *model-independent* reflects borrowing from the best parts of both model-dependent selection and model-free variable selection in the literature. This is because we construct trees just like in permutation importance and tree filtering methods, but our goal is different: to obtain rules and regions of the feature space over which to calculate our importance score, rather than using predicted outcomes and prediction error to determine importance. In this paper, we are interested in developing a consistent model-independent rule-based variable selection procedure applicable across different data settings.

Let Y be the response variable and $X^{(1)}, \dots, X^{(p)}$ the set of p potential explanatory features. We consider the setting where the researcher is interested in the conditional distribution of the response Y given the features $\mathbf{X} = (X^{(1)}, \dots, X^{(p)})$. Our goal is to identify the variables of importance for a given function of the conditional distribution of Y given \mathbf{X} . We call the target of interest $\psi(\mathbf{X}) = \mathbb{E}(g(Y)|\mathbf{X})$, where g is a prechosen function specific to the problem being studied. Some examples are given below:

1. *Regression.* Here $\psi(\mathbf{X}) = \mathbb{E}(Y|\mathbf{X})$ where $g(Y) = Y$ and the goal is determining variables affecting the conditional mean.
2. *Classification.* For a categorical response with categories c_1, \dots, c_L , interest could focus on the conditional probability $\psi(\mathbf{X}) = \mathbb{P}\{Y = c_l|\mathbf{X}\}$ for a specific category c_l , where $g(Y) = I\{Y = c_l\}$. For example, in studying the presence, absence, or recurrence of cancer, the researcher may focus on the recurrence of cancer to study the hypothesis that the probability of recurrence depends on certain features.
3. *Time to event.* With survival analysis, the focus of interest can be the survival function $\psi(\mathbf{X}) = \mathbb{P}\{T^o > t|\mathbf{X}\}$, where $Y = T^o$ is the survival time. In this case, $g(T^o) = I\{T^o > t\}$.

Since it is expected that ψ will depend on a smaller subset of the p variables $\mathcal{S} \subset \{1, \dots, p\}$, the task is to find the minimal set \mathcal{S} for which this holds, which we call the “signal variables”, while simultaneously excluding the non-relevant variables, which we call “noise variables”. To make this idea more precise we provide the following definition. Write $\mathbf{X}^{(S)} = \{X^{(j)}\}_{j \in S}$ for the feature vector \mathbf{X} restricted to coordinates $j \in S$ and $\mathbf{X}^{\setminus(S)} = \{X^{(j)}\}_{j \notin S}$ for coordinates not in S .

DEFINITION 1.1. $\mathcal{S} \subset \{1, \dots, p\}$ is the set of signal variables if \mathcal{S} is the minimal set of coordinates that ψ depends on. Thus, \mathcal{S} is the smallest subset of coordinates satisfying $\mathbb{P}\{\psi(\mathbf{X}) = \psi(\mathbf{X}^{(S)})\} = 1$ such that $\mathbb{P}\{\psi(\mathbf{X}^{(S)}) = \psi(\mathbf{X}^{(S')})\} = 0$ for every S' where $S \not\subseteq S'$. The complementary set $\mathcal{N} = \{1, \dots, p\} \setminus \mathcal{S}$ is unrelated to ψ and therefore contains the noise variables. If $\mathcal{S} = \emptyset$, then $\psi = \mathbb{E}(g(Y))$ is constant and $\mathcal{N} = \{1, \dots, p\}$. However, we rule this trivial case out and always assume $\mathcal{S} \neq \emptyset$.

The definition of \mathcal{S} specifies that it is the smallest set of coordinates such that $\psi(\mathbf{x}) = \psi(\mathbf{x}^{(S)})$ for almost all \mathbf{x} . Furthermore, there is no other set $S' \neq \mathcal{S}$ (where $\mathcal{S} \not\subseteq S'$) for which

$\psi(\mathbf{X}) = \psi(\mathbf{X}^{(S)})$ holds with non-zero probability. Another way to view [Definition 1.1](#) is that it implies a type of conditional independence for noise variables. For example, if $p = 2$ and $\mathcal{S} = \{1\}$, then since $X^{(2)}$ is a noise variable

$$\mathbb{E}\left(g(Y)|X^{(1)}, X^{(2)}\right) = \mathbb{E}\left(g(Y)|X^{(1)}\right). \quad (1)$$

We note (1) is weaker than the usual conditional independence assumption used for variable selection (see equation (2) below) since it depends upon the choice of g and ψ . For example, in classification, if the analysts chooses $g(Y) = I\{Y = c_l\}$ for a specific class label c_l of interest, (1) implies a conditional independence of $X^{(2)}$ for class label c_l , but not necessarily for other class labels. Thus, variables affecting relapse of cancer may be different from those affecting absence or death due to cancer. The ability to select (g, ψ) to suit the data question being studied is an important feature of our approach and provides researchers with a flexible tool to study how variables play a role in their data settings. As another example, consider survival analysis. As discussed in Section 5, a useful way to summarize lifetime behavior is by restricted mean survival time (RMST) [56]. The RMST equals the integrated survival function up to a fixed time horizon value $\tau > 0$ and equals

$$\psi_\tau(\mathbf{X}) = \int_0^\tau \mathbb{P}\{T^o > t|\mathbf{X}\} dt = \mathbb{E}(g(T^o)|\mathbf{X}), \quad \text{where } g(T^o) = T^o \wedge \tau.$$

Because $\psi_\tau(\mathbf{X})$ can vary with time, the list of signal variables can vary with τ . For example, identifying variables affecting year one breast cancer survival is crucial for properly managing early treatment, but knowing which variables affect lifetime after year one is equally important for tailoring treatment for long-term survival.

Our approach works with the function ψ obtained by integration with respect to the conditional distribution of Y given \mathbf{X} , but another method often used is to work directly with the conditional distribution. This assumes a conditional independence between Y and the noise variables given the signal variables:

$$Y \perp \mathbf{X}^{(S)} | \mathbf{X}^{(S)}. \quad (2)$$

Let $S \subset \{1, \dots, p\}$ be the variables of interest, and the goal is to determine if S contains signal variables. The strategy is to construct a test statistic $\hat{\theta}_n(S)$ using augmented features $(\mathbf{X}^{(S)}, \mathbf{X}^{(S)}, \tilde{\mathbf{X}}^{(S)}, \tilde{\mathbf{X}}^{(S)})$, where $\tilde{\mathbf{X}}^{(S)}$ and $\tilde{\mathbf{X}}^{(S)}$ are new artificial features. The test is constructed in such a way that, due to conditional independence, $\hat{\theta}_n(S)$ is statistically non-significant if S are noise variables.

We mention two popular methods using this idea. The first is permutation importance for random forests mentioned earlier (referred to hereafter as VIMP for variable importance). In VIMP, the feature vector $\mathbf{X}^{(S)}$ is permuted to obtain $\tilde{\mathbf{X}}^{(S)}$; then the predicted value for $(\mathbf{X}^{(S)}, \mathbf{X}^{(S)})$ is compared to the predicted value for $(\mathbf{X}^{(S)}, \tilde{\mathbf{X}}^{(S)})$, where this difference should be nearly zero if (2) holds. However, a well-known problem with VIMP is that the permuted sample does not have the same distribution as \mathbf{X} , which can lead to flawed variable selection [61]. The second technique is knockoffs [8]. In knockoffs, a simulation according to the distribution of \mathbf{X} is used to obtain $(\tilde{\mathbf{X}}^{(S)}, \tilde{\mathbf{X}}^{(S)})$, where the artificial data is simulated so as to satisfy

$$(\mathbf{X}^{(S)}, \mathbf{X}^{(S)}, \tilde{\mathbf{X}}^{(S)}, \tilde{\mathbf{X}}^{(S)}) \stackrel{d}{=} (\mathbf{X}^{(S)}, \tilde{\mathbf{X}}^{(S)}, \tilde{\mathbf{X}}^{(S)}, \mathbf{X}^{(S)}). \quad (3)$$

This is used to compute a knockoff statistic for filtering variables. By making use of (2), the knockoff test statistic can achieve a desired false discovery level. This novel idea avoids the problems of permutation importance; however, it may rely on strong assumptions about the parent distribution, and achieving (3) could be difficult in certain situations.

1.1. *Contributions of this work and outline of the paper.* The VarPro method introduces a novel approach to using rules. A similar method is the mean decrease impurity (MDI) score [7]. For a given variable $X^{(s)}$, the MDI score is obtained by summing the weighted impurity decrease across all tree nodes that involve a split using $X^{(s)}$ [for forests, the MDI is averaged over all trees in the forest; see 51]. This score provides a useful summary of a feature’s importance and is used for ranking variables. When the Gini index is used as the impurity function in classification, this measure is known as the Gini importance. VarPro can be viewed as a generalization of MDI since MDI is approximately recovered in the proposed framework when setting g to either the Gini index for classification or the variance in regression. However, VarPro extends MDI because the VarPro importance score for a feature is determined by a local estimator *that drops all conditions on the feature at once*, whereas MDI considers the marginal effect of the feature (i.e., the impurity drop at a specific node that splits on $X^{(s)}$).

The structure of the paper is as follows. Section 2 describes the VarPro procedure in detail. Given a rule, the VarPro importance score for a set of variables S is defined as the difference between two local estimators of ψ , where one is estimated from the region of the data defined by the rule and the other by removing any constraints on the rule involving the features in S . The local estimators are simple averages of statistics and are relatively easy to calculate. Examples are provided to motivate the method and explain the concepts of a region and its released region, which are essential to understanding the VarPro importance score. We then contrast VarPro with permutation importance to highlight its advantages. In this discussion, we find that VarPro can be written as a permutation test, allowing us to pinpoint the shortcomings of permutation importance and demonstrate how VarPro overcomes these issues.

Section 3 provides theoretical justification for VarPro. Our theory considers both the null case, when the variable is noise, and the alternative case, when the variable has signal. We show that VarPro consistently filters out noise variables and, for signal variables, we derive the asymptotic limit of a bias term representing the limiting VarPro importance score. These results hold under relatively mild conditions, such as a smoothness property for ψ and certain conditions for the rules used by VarPro. These conditions are expected to hold for any reasonably constructed tree procedure, making VarPro generally agnostic to the rule-based procedure used for rule generation.

Section 4 presents empirical results demonstrating VarPro’s effectiveness using synthetic and real-world data for regression and classification in both low and high-dimensional feature spaces. Building on the work in Section 2, we extend VarPro to survival analysis in Section 5. A large cardiovascular study and high-dimensional simulations are used to illustrate the effectiveness of this extension. Section 6 concludes with a discussion summarizing the strengths and weaknesses of the method. All proofs and supplementary information are located in the Appendix.

2. A new rule-based variable selection approach. We begin by providing a broad overview of the idea, after which we will delve into specific details. Let S again represent the set of variables of interest. Given a rule ζ , VarPro calculates a sample averaged estimator $\hat{\theta}_n(\zeta)$ for the target function ψ of interest by using the data in ζ ’s *region*. Then a *released rule* ζ^S is constructed by removing any constraints on the indices in S , and its sample averaged estimator $\hat{\theta}_n(\zeta^S)$ is calculated over the *released region*. The estimator $\hat{\theta}_n(\zeta^S)$ is then contrasted with $\hat{\theta}_n(\zeta)$ to measure the importance of S . Many existing methods for variable importance rely on either resampling or refitting models, which can introduce finite sample bias, or they make use of artificial data as described earlier. A unique feature of VarPro is that it bypasses the need for this, and instead constructs estimators $\hat{\theta}_n(\zeta)$ and $\hat{\theta}_n(\zeta^S)$ directly

from the data. These estimators serve as local estimates of ψ , and because $\hat{\theta}_n(\zeta^S)$ is calculated using the data from releasing coordinates on S , it implies under certain conditions due to the laws of averages that $|\hat{\theta}_n(\zeta) - \hat{\theta}_n(\zeta^S)| \xrightarrow{P} 0$ for noise variables S . However, for signal variables, the limit is different. Therefore, this makes it possible to consistently filter noise variables using the VarPro importance score $|\hat{\theta}_n(\zeta) - \hat{\theta}_n(\zeta^S)|$.

2.1. Regions and release regions. A key aspect of VarPro is the idea of the region of a rule ζ . A region is a subset of the feature space obtained by a function R that maps $\zeta \mapsto \mathcal{X}$. In many cases, ζ can be associated with a series of univariate rules. The region mapped by R in this case is denoted by $R(\zeta) = \{\mathbf{x} \in \mathcal{X} : x^{(1)} \in R(\zeta^{X^{(1)}}), \dots, x^{(p)} \in R(\zeta^{X^{(p)}})\}$, where $\zeta^{X^{(j)}}$ denotes the univariate rule for feature j . For example, if all the features are continuous, we can imagine a rule with region $R(\zeta) = \{\mathbf{x} \in \mathbb{R}^p : a_1 \leq x^{(1)} \leq b_1, \dots, a_p \leq x^{(p)} \leq b_p\}$. Boundaries like this naturally arise in machine learning methods constructed from decision rules.

In order to construct the VarPro importance score we need to introduce the idea of a released rule and a released region.

DEFINITION 2.1. *Let $R(\zeta) \subset \mathcal{X}$ be a region of the feature space. To check the importance of the variables $\mathbf{X}^{(S)}$ to the rule ζ , we introduce the concept of a released region $R(\zeta^S)$ for the released rule ζ^S obtained by removing the dependence of ζ on the coordinates $\mathbf{X}^{(S)}$:*

$$R(\zeta^S) = \{\mathbf{x} \in \mathcal{X} : \mathbf{x}^{\setminus(S)} \in R(\zeta)\}.$$

In other words, the released region $R(\zeta^S)$ is the set of all \mathbf{x} whose S -coordinate values are unconstrained but with non- S -coordinate values that lie in $R(\zeta)$. In particular, $R(\zeta) \subseteq R(\zeta^S)$.

Example 1. In this example, shown in Fig. 1, the feature space is $\mathcal{X} \subseteq \mathbb{R}^2$ and the rule ζ corresponds to the branch of a tree using splits $x^{(1)} \leq -0.7$, $x^{(2)} \geq -0.8$, $x^{(2)} \leq 0.7$, and $x^{(1)} \geq -1.95$. We can think of ζ as a product of indicator functions:

$$\zeta = I\{x^{(1)} \leq -0.7\} \cdot I\{x^{(2)} \geq -0.8\} \cdot I\{x^{(2)} \leq 0.7\} \cdot I\{x^{(1)} \geq -1.95\}.$$

The region $R(\zeta)$ is the blue rectangle in Fig. 1 (A):

$$R(\zeta) = \{(x^{(1)}, x^{(2)}) : -1.95 \leq x^{(1)} \leq -0.7, -0.8 \leq x^{(2)} \leq 0.7\}.$$

Consider testing whether $X^{(2)}$ is a noise variable. Then, by Definition 2.1, we set $S = \{2\}$ and obtain the released region by removing the dependence on coordinate $X^{(2)}$:

$$R(\zeta^S) = \{(x^{(1)}, x^{(2)}) : -1.95 \leq x^{(1)} \leq -0.7\}.$$

The released region is therefore the rectangle with the sides for the released coordinates removed (see the pink region in Fig. 1 (C)). Interestingly, since we are working with a classical tree, the released rule is itself a tree branch equal to the original rule altered such that whenever a binary decision is made on a variable in S , the decision is always 1. In this example, $\zeta^S = I\{x^{(1)} \leq -0.7\} \cdot I\{x^{(1)} \geq -1.95\}$. \square

Example 2. Fig. 2 illustrates how Definition 2.1 can apply to rules other than those from classical trees. In both illustrations, the region of interest is a function of the variables that is not decomposable into products of conditions on individual variables as in a typical tree. The top left panel shows an elliptical region, which is a rule condition given by a quadratic inequality relating to both variables. According to Definition 2.1, to release the region along

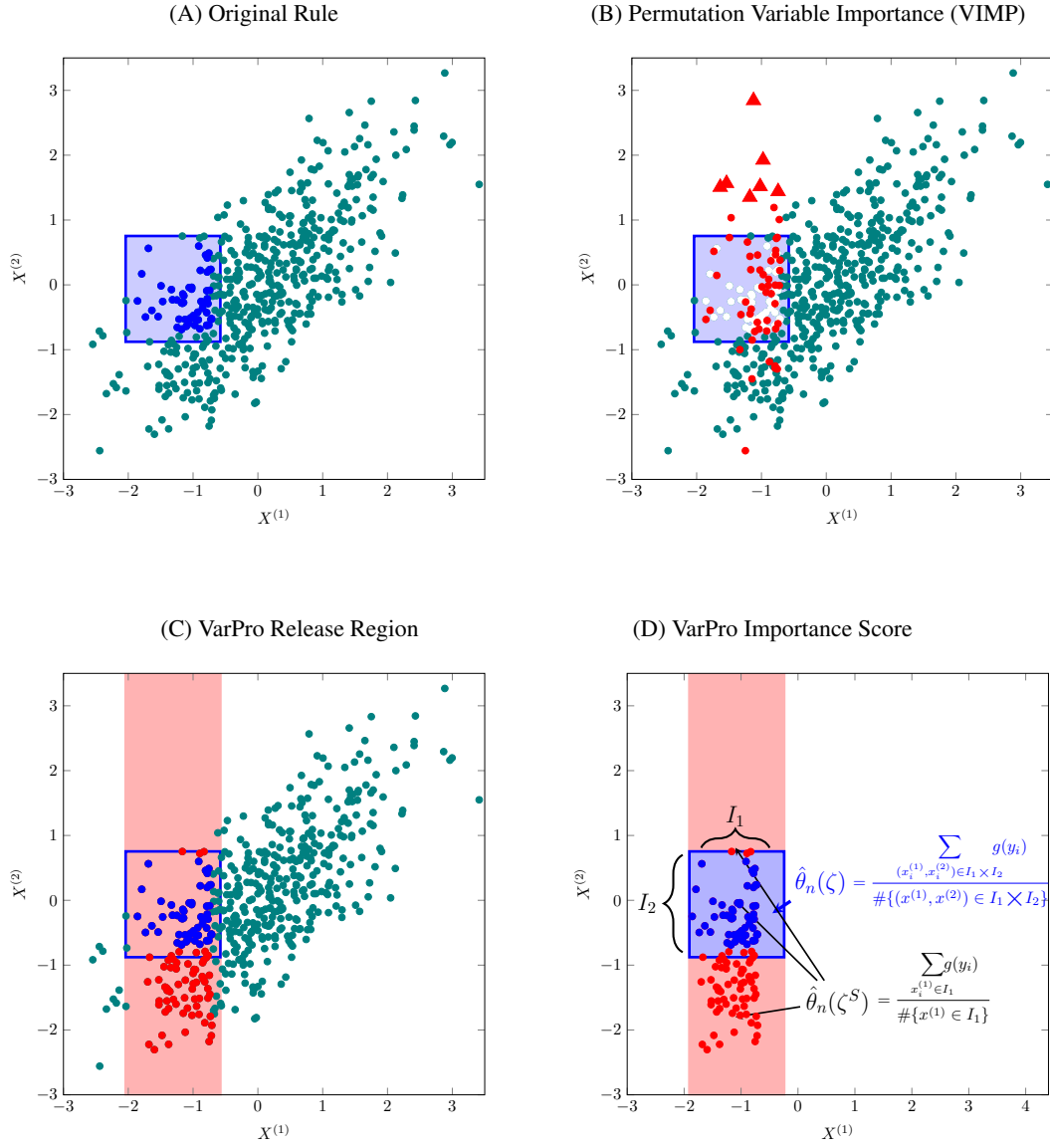


FIG 1. Two-dimensional illustration of how VarPro differs from artificial data methods. (A) The two-dimensional region for ζ is a rectangle. The data of interest are marked in blue. (B) Permutation variable importance (VIMP) for $X^{(2)}$. The data was permuted along $X^{(2)}$ and data marked in red with triangles identify values that do not match the joint distribution of \mathbf{X} . The model-based predicted values $\tilde{y} := \tilde{y}(x^{(1)}, \tilde{x}^{(2)})$ for these artificial points are extrapolated from a region of the feature space that could be from potentially different responses. (C) VarPro release region for $X^{(2)}$. The original rule is modified to the S -released rule ζ^S (where $S = \{2\}$) shown using a pink background color. (D) VarPro importance score is defined using the estimator calculated using observed data values in blue compared to the estimator where the new released values in red are additionally used. No artificial data needs to be created.

$X^{(2)}$, we take the set of all \mathbf{x} with coordinates $X^{(1)}$ inside the ellipse, while $X^{(2)}$ is left unconstrained. Therefore, the released region $R(\zeta^S)$ is a box that touches the left and right sides of the ellipse as shown in the top middle panel. The panel to its right shows the release region when $X^{(1)}$ is released. This is a box that touches the top and bottom of the ellipse. The second illustration, given in the bottom left of Fig. 2, is a hyperplane region. This is a rule condition given by a simple linear inequality condition relating to both variables (for instance, this would occur for rules extracted from random projection trees). The middle and right bottom panels display the release region when releasing coordinates $X^{(2)}$ and $X^{(1)}$. Observe that in both of our examples, the released rule ζ^S obtained by releasing S may not correspond to a rule generated by the original machine learning procedure. This is because if the region is a function that depends on the features using some type of threshold function, then the resulting rule may be different from the rules generated by the original procedure. Nonetheless, our framework is designed to accommodate such a scenario. \square

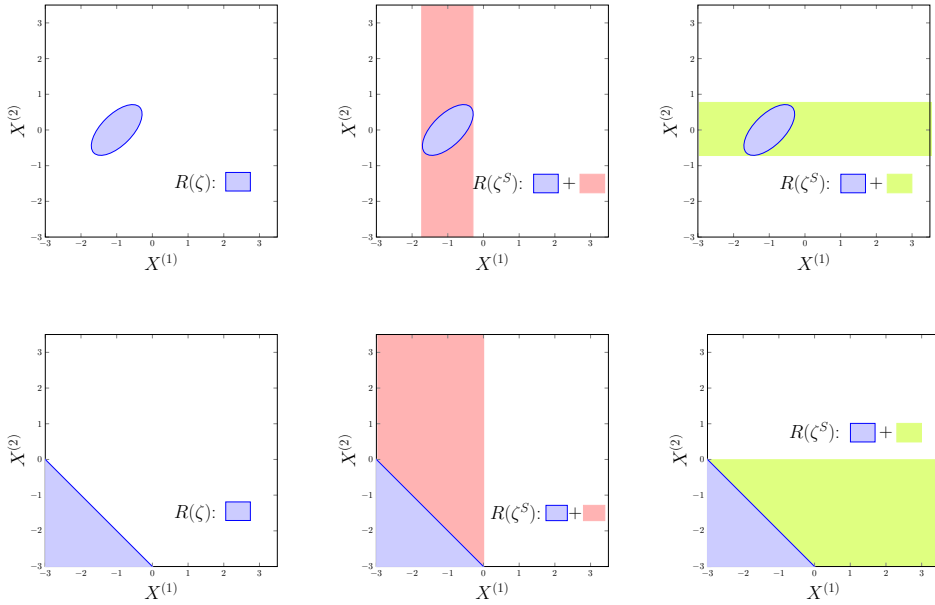


FIG 2. Regions $R(\zeta)$ (in blue) for rules ζ produced by a machine learning procedure. Top left is for an elliptical rule; bottom left is for a hyperplane rule. Middle and right column figures are release region $R(\zeta^S)$ when releasing coordinates $X^{(2)}$ with $S = \{2\}$ (red plus blue region) and $X^{(1)}$ with $S = \{1\}$ (green plus blue region), respectively.

2.2. VarPro importance score. The VarPro importance score is defined formally as follows. Let $(\mathbf{X}_1, Y_1), \dots, (\mathbf{X}_n, Y_n) \in \mathcal{X} \times \mathcal{Y}$ be the i.i.d. learning data sampled from \mathbb{P} . Observations Y_i for $\mathbf{X}_i \in R(\zeta)$ are used to estimate the conditional mean of $g(Y)$ in $R(\zeta)$ via

$$\hat{\theta}_n(\zeta) = \frac{1}{\#\{\mathbf{X}_i \in R(\zeta)\}} \sum_{\mathbf{X}_i \in R(\zeta)} g(Y_i). \quad (4)$$

The released region $R(\zeta^S)$ is used to obtain the released estimator

$$\hat{\theta}_n(\zeta^S) = \frac{1}{\#\{\mathbf{X}_i \in R(\zeta^S)\}} \sum_{\mathbf{X}_i \in R(\zeta^S)} g(Y_i). \quad (5)$$

The VarPro importance of S is defined as the absolute difference between (4) and (5), $|\hat{\theta}_n(\zeta^S) - \hat{\theta}_n(\zeta)|$.

We return to our previous example of Fig. 1 to give some intuition for this estimator by contrasting it to permutation importance (VIMP). Recall that $R(\zeta)$ is the blue rectangle in (A) and the released region $R(\zeta^S)$ is the pink area in (C). Panel (B) displays the data after permutation on coordinate $X^{(2)}$. Permuted data $(x^{(1)}, \tilde{x}^{(2)}) \in R(\zeta^S)$ are marked in red. Notice that in some cases (indicated by triangles) these data deviate strongly from the true distribution of $(X^{(1)}, X^{(2)})$. This creates problems for VIMP. This is because VIMP calculates the importance of $X^{(2)}$ by comparing the test statistic calculated using the observed data in $R(\zeta)$ (blue points in (A)) to that calculated using the permuted data in $R(\zeta^S)$ (red points in (B)). If this were a regression setting, this corresponds to averaging observations y_i for $i \in R(\zeta)$ and comparing them to averaged estimated values $\tilde{y}_i := \tilde{y}_i(x_i^{(1)}, \tilde{x}_i^{(2)})$. Unfortunately, since \tilde{y}_i has to be model estimated (since it must estimate ψ for features not in the training data), this produces atypical \tilde{y}_i if $\tilde{x}_i^{(2)}$ is from a different region of the data space than the original data (like the red triangular points). This can result in large VIMP even when $X^{(2)}$ is a noise variable.

This problem occurs because the learner is being applied to artificially created data that deviates from the feature distribution. To avoid this, VarPro takes a direct approach. Using the original training data, estimates are obtained for the conditional mean of $g(Y)$ for $\mathbf{X} \in R(\zeta)$ using observed values $g(y_i)$ via (4) and (5), where in a regression setting $g(y) = y$. Shown in Fig. 1 (D), $\hat{\theta}_n(\zeta)$ is calculated from observations in the blue box (blue points), which is compared to $\hat{\theta}_n(\zeta^S)$ calculated using the data in the pink rectangle (blue and red points), yielding the importance value

$$\left| \hat{\theta}_n(\zeta^S) - \hat{\theta}_n(\zeta) \right| = \left| \frac{\sum_{x_i^{(1)} \in I_1} y_i}{\#\{x^{(1)} \in I_1\}} - \frac{\sum_{(x_i^{(1)}, x_i^{(2)}) \in I_1 \times I_2} y_i}{\#\{(x^{(1)}, x^{(2)}) \in I_1 \times I_2\}} \right|,$$

where $I_1 = [-1.95, -0.7]$ and $I_2 = [-.8, 0.7]$. If $X^{(1)}$ is a signal feature, but $X^{(2)}$ is a noise variable, then the two averages should converge to nearly the same value because $\psi(\mathbf{X}) = \mathbb{E}(Y|\mathbf{X}) = \psi(X^{(1)})$ depends only on $X^{(1)}$. On the other hand, if $X^{(2)}$ is a signal feature, then the difference will not necessarily be zero.

VARPRO KEY IDEA. *Releasing a rule ζ along the noise coordinates does not change ψ , therefore the difference between the average of g in the rule's region and its released region will be asymptotically the same, and subsequently we can expect a zero importance. For signal variables, the opposite happens, and since ψ changes along the released direction, we can expect a difference in average g values in the released and non-released regions, and therefore we can expect a non-zero importance value asymptotically.*

2.3. Connection of VarPro to permutation tests. We use the following construction to gain insight into the dangers of using artificial data as well as to expand on our previous points about VIMP. Surprisingly, it turns out that we can write the VarPro estimator as a specialized type of permutation test. This will be contrasted against model-based importance to explain what goes wrong with artificial data and to explain how VarPro avoids this. This also motivates the idea of using an external estimator to be used in Section 5 for survival analysis.

Without loss of generality, assume that \mathbf{x} is reordered so that $\mathbf{x} = (\mathbf{x}^{(S)}, \mathbf{x}^{\setminus(S)})$. Consider all possible permutations of the training data $\{(y_i, \mathbf{x}_j^{(S)}, \mathbf{x}_i^{\setminus(S)})\}_{1 \leq i, j \leq n}$. Then it will be shown

(see below) that

$$\frac{\sum_{i=1}^n g(y_i) I\{\mathbf{x}_i \in R(\zeta^S)\}}{\sum_{i=1}^n I\{\mathbf{x}_i \in R(\zeta^S)\}} = \frac{\sum_{i=1}^n \sum_{j=1}^n g(y_i) I\{(\mathbf{x}_j^{(S)}, \mathbf{x}_i^{\setminus(S)}) \in R(\zeta)\}}{\sum_{i=1}^n \sum_{j=1}^n I\{(\mathbf{x}_j^{(S)}, \mathbf{x}_i^{\setminus(S)}) \in R(\zeta)\}}. \quad (6)$$

The left-hand side is the VarPro released estimator $\hat{\theta}_n(\zeta^S)$ described in (5), whereas the right-hand side is an estimator using the permuted data. Obviously in practice the permuted estimator on the right side of (6) is impractical since it involves $O(n^2)$ calculations and would be an inefficient way to calculate $\hat{\theta}_n(\zeta^S)$. However, we use it to describe why permutation VIMP generally does not satisfy an identity like (6), which will highlight the problem.

First, however, let us explain why (6) holds. Let $\zeta^{\setminus(S)}$ be the rule that relaxes the constraints of ζ on the indices not in S . We have the following identity for rules expressible as products $\zeta = \prod_{s=1}^p I\{x^{(s)} \in I_s\}$ where $I_s \subseteq \mathbb{R}$ are real-valued intervals (this is like the example described in Fig. 1):

$$I\{\mathbf{x} \in R(\zeta)\} = I\{\mathbf{x}^{\setminus(S)} \in R(\zeta)\} \cdot I\{\mathbf{x}^{(S)} \in R(\zeta)\} = I\{\mathbf{x} \in R(\zeta^S)\} \cdot I\{\mathbf{x} \in R(\zeta^{\setminus(S)})\}. \quad (7)$$

The right side follows by Definition 2.1 since $\mathbf{x} \in R(\zeta^S)$ implies $\mathbf{x}^{\setminus(S)} \in R(\zeta)$ and $\mathbf{x} \in R(\zeta^{\setminus(S)})$ implies $\mathbf{x}^{(S)} \in R(\zeta)$ and vice-versa.

Therefore, for rules satisfying (7)

$$\begin{aligned} I\{(\mathbf{x}_j^{(S)}, \mathbf{x}_i^{\setminus(S)}) \in R(\zeta)\} &= I\{(\mathbf{x}_j^{(S)}, \mathbf{x}_i^{\setminus(S)}) \in R(\zeta^S)\} \cdot I\{(\mathbf{x}_j^{(S)}, \mathbf{x}_i^{\setminus(S)}) \in R(\zeta^{\setminus(S)})\} \\ &= I\{\mathbf{x}_i \in R(\zeta^S)\} \cdot I\{\mathbf{x}_j \in R(\zeta^{\setminus(S)})\} \end{aligned} \quad (8)$$

where the last line is because $(\mathbf{x}_j^{(S)}, \mathbf{x}_i^{\setminus(S)}) \in R(\zeta^S)$ depends only on $\mathbf{x}_i^{\setminus(S)}$ and $(\mathbf{x}_j^{(S)}, \mathbf{x}_i^{\setminus(S)}) \in R(\zeta^{\setminus(S)})$ depends only on $\mathbf{x}_j^{(S)}$. Hence we have

$$\begin{aligned} &\frac{\sum_{i=1}^n \sum_{j=1}^n g(y_i) I\{(\mathbf{x}_j^{(S)}, \mathbf{x}_i^{\setminus(S)}) \in R(\zeta)\}}{\sum_{i=1}^n \sum_{j=1}^n I\{(\mathbf{x}_j^{(S)}, \mathbf{x}_i^{\setminus(S)}) \in R(\zeta)\}} \\ &= \frac{\sum_{i=1}^n \sum_{j=1}^n g(y_i) I\{\mathbf{x}_i \in R(\zeta^S)\} I\{\mathbf{x}_j \in R(\zeta^{\setminus(S)})\}}{\sum_{i=1}^n \sum_{j=1}^n I\{\mathbf{x}_i \in R(\zeta^S)\} I\{\mathbf{x}_j \in R(\zeta^{\setminus(S)})\}} \\ &= \frac{\sum_{i=1}^n g(y_i) I\{\mathbf{x}_i \in R(\zeta^S)\} \sum_{j=1}^n I\{\mathbf{x}_j \in R(\zeta^{\setminus(S)})\}}{\sum_{i=1}^n I\{\mathbf{x}_i \in R(\zeta^S)\} \sum_{j=1}^n I\{\mathbf{x}_j \in R(\zeta^{\setminus(S)})\}} \\ &= \frac{\sum_{i=1}^n g(y_i) I\{\mathbf{x}_i \in R(\zeta^S)\}}{\sum_{i=1}^n I\{\mathbf{x}_i \in R(\zeta^S)\}} := \hat{\theta}_n(\zeta^S). \end{aligned}$$

The first line is from (8). The last line is due to the cancellation of the common term in the numerator and denominator which is directly related to working with $g(y_i)$.

Now let us compare this to VIMP. Recall that unlike VarPro, VIMP does not use the observed response to estimate ψ but uses a model-based estimator instead. Let ψ_n be this estimator. For example, this could be the ensemble estimator from a random forest analysis or a tree boosted estimator using gradient boosting. Then using the permuted data as above, the VIMP estimator is

$$\begin{aligned} \tilde{\theta}_{\text{VIMP}}(\zeta^S) &= \frac{\sum_{i=1}^n \sum_{j=1}^n \psi_n(\mathbf{x}_j^{(S)}, \mathbf{x}_i^{\setminus(S)}) I\{(\mathbf{x}_j^{(S)}, \mathbf{x}_i^{\setminus(S)}) \in R(\zeta)\}}{\sum_{i=1}^n \sum_{j=1}^n I\{(\mathbf{x}_j^{(S)}, \mathbf{x}_i^{\setminus(S)}) \in R(\zeta)\}} \\ &= \frac{\sum_{i=1}^n \sum_{j=1}^n \psi_n(\mathbf{x}_j^{(S)}, \mathbf{x}_i^{\setminus(S)}) I\{\mathbf{x}_i \in R(\zeta^S)\} I\{\mathbf{x}_j \in R(\zeta^{\setminus(S)})\}}{\sum_{i=1}^n I\{\mathbf{x}_i \in R(\zeta^S)\} \sum_{j=1}^n I\{\mathbf{x}_j \in R(\zeta^{\setminus(S)})\}} \end{aligned}$$

where the last identity is due to (8).

Notice, however, that the cancellation that occurred previously in the numerator and denominator is no longer guaranteed to hold, and it is not true that $\theta_{\text{VIMP}}(\zeta^S)$ is the same as the non-permuted estimator

$$\tilde{\theta}_n(\zeta^S) = \frac{\sum_{i=1}^n \psi_n(\mathbf{x}_i) I\{\mathbf{x}_i \in R(\zeta^S)\}}{\sum_{i=1}^n I\{\mathbf{x}_i \in R(\zeta^S)\}}, \quad (9)$$

which is the analog to $\hat{\theta}_n(\zeta^S)$ since it replaces the observed value $g(y_i)$ with the model estimated value $\psi_n(\mathbf{x}_i)$. Just like $\hat{\theta}_n(\zeta^S)$, the estimator $\tilde{\theta}_n(\zeta^S)$ leads to consistent variable selection (to be shown in [Theorem 5.1](#)) so the equality would show that the model-based permutation importance has good properties. But this cancellation occurs and the two estimators become the same only if

$$\psi_n(\mathbf{x}) = \psi_n(\mathbf{x}^{\setminus(S)}) \quad (10)$$

because then

$$\begin{aligned} \tilde{\theta}_{\text{VIMP}}(\zeta^S) &= \frac{\sum_{i=1}^n \psi_n(\mathbf{x}_i^{\setminus(S)}) I\{\mathbf{x}_i \in R(\zeta^S)\} \sum_{j=1}^n I\{\mathbf{x}_j \in R(\zeta^{\setminus(S)})\}}{\sum_{i=1}^n I\{\mathbf{x}_i \in R(\zeta^S)\} \sum_{j=1}^n I\{\mathbf{x}_j \in R(\zeta^{\setminus(S)})\}} \\ &= \frac{\sum_{i=1}^n \psi_n(\mathbf{x}_i^{\setminus(S)}) I\{\mathbf{x}_i \in R(\zeta^S)\}}{\sum_{i=1}^n I\{\mathbf{x}_i \in R(\zeta^S)\}} := \tilde{\theta}_n(\zeta^S). \end{aligned}$$

However (10) is a very strong assumption. If S consists entirely of noise variables then $\psi(\mathbf{x}) = \psi(\mathbf{x}^{\setminus(S)})$, so in this case (10) is asserting that the model-based estimator has correctly eliminated all noise variables. This is a very strong requirement and is asking a lot from the underlying procedure since after all this would mean that the procedure has achieved perfect variable selection on its own. Therefore, it is not reasonable to expect (10) to hold in general, which means $\tilde{\theta}_{\text{VIMP}}(\zeta^S)$ will not equal $\tilde{\theta}_n(\zeta^S)$ in general.

We emphasize that while this highlights the issue of using ψ_n with $\tilde{\theta}_{\text{VIMP}}(\zeta^S)$, this does not necessarily detract from the potential usefulness of an external estimator. A point we explore is how to use the external estimator in a more coherent way. We argue that the non-permuted estimator $\tilde{\theta}_n(\zeta^S)$ defined in (9) presents one such opportunity. After all, we know that machine learning methods like gradient boosting and random forests produce highly accurate estimators in many settings. VIMP misuses ψ_n by applying it to artificial data, which can produce biased estimation. However, the non-permuted estimator $\tilde{\theta}_n(\zeta^S)$, which was introduced as an analog to the VarPro estimator, only applies ψ_n to the training data. This is why it does not equal permutation VIMP and why it represents a legitimate way to proceed.

In fact, in Section 5 we develop an estimator like this for survival analysis to extend VarPro to handle censored data. As will be discussed, in censored settings an external estimator makes sense. However at the same time, if the response is observed, then we prefer to use the VarPro importance score

$$\left| \hat{\theta}_n(\zeta^S) - \hat{\theta}_n(\zeta) \right| = \left| \frac{\sum_{i=1}^n g(y_i) I\{\mathbf{x}_i \in R(\zeta^S)\}}{\sum_{i=1}^n I\{\mathbf{x}_i \in R(\zeta^S)\}} - \frac{\sum_{i=1}^n g(y_i) I\{\mathbf{x}_i \in R(\zeta)\}}{\sum_{i=1}^n I\{\mathbf{x}_i \in R(\zeta)\}} \right|$$

which is model-independent and makes use of the actual observed responses, rather than an external importance score

$$\left| \tilde{\theta}_n(\zeta^S) - \tilde{\theta}_n(\zeta) \right| = \left| \frac{\sum_{i=1}^n \psi_n(\mathbf{x}_i) I\{\mathbf{x}_i \in R(\zeta^S)\}}{\sum_{i=1}^n I\{\mathbf{x}_i \in R(\zeta^S)\}} - \frac{\sum_{i=1}^n \psi_n(\mathbf{x}_i) I\{\mathbf{x}_i \in R(\zeta)\}}{\sum_{i=1}^n I\{\mathbf{x}_i \in R(\zeta)\}} \right|$$

which is model-specific. The former leads to a simpler procedure based on averages of independent observations which is consistent under relatively mild conditions. Also it is easier to apply to different g functions without having to fit a new learning method when g is changed by the researcher.

3. Theory. How does one construct a rule ζ to identify variables informative for ψ ? In practice, there are many procedures to choose from that produce rules for VarPro, including simple decision rules [62], rule learning [21], trees [7], Bayesian trees [52], Bayesian additive regression trees [11], Bayesian forests [50] and random forests [5]. In the examples presented in this paper, the rules are chosen by randomly selecting branches from a CART tree.

We assume hereafter that we have constructed a rule, or more generally, a collection of rules for a specific problem. Previously we had defined the VarPro importance score on the basis of a single rule, but we will actually use many rules and average their scores to obtain a more stable estimator (see the discussion following [Theorem 3.2](#) for an explanation for why more rules improve stability). The rules are assumed to be constructed independently of the data used by VarPro, and therefore without loss of generality, it will be assumed that all rules are deterministic. For each n , let $\zeta_{n,1}, \dots, \zeta_{n,K_n}$ denote these rules. Notice that the number of rules K_n can vary with n and also that the rules themselves are allowed to change with n . For a given rule ζ , define

$$\hat{\theta}_n(\zeta) = m_n(\zeta)^{-1} \sum_{i=1}^n g(Y_i) I\{\mathbf{X}_i \in R(\zeta)\}, \quad m_n(\zeta) = \sum_{i=1}^n I\{\mathbf{X}_i \in R(\zeta)\},$$

which is a slightly more compact way of writing $\hat{\theta}_n$ than (4) (notice that $m_n(\zeta)$ equals the sample size of a rule ζ). In a likewise fashion, we can define $\hat{\theta}_n(\zeta^S) = m_n(\zeta^S)^{-1} \sum_{i=1}^n g(Y_i) I\{\mathbf{X}_i \in R(\zeta^S)\}$.

For notational ease, let $m_{n,k} = m_n(\zeta_{n,k})$, $m_{n,k}^S = m_n(\zeta_{n,k}^S)$ and $R_{n,k} = R(\zeta_{n,k})$, $R_{n,k}^S = R(\zeta_{n,k}^S)$. The VarPro importance score for S is defined as the weighted averaged difference

$$\begin{aligned} \Delta_n(S) &= \sum_{k=1}^{K_n} W_{n,k} |\hat{\theta}_n(\zeta_{n,k}^S) - \hat{\theta}_n(\zeta_{n,k})| \\ &= \sum_{k=1}^{K_n} W_{n,k} \left| \frac{1}{m_{n,k}^S} \sum_{i=1}^n g(Y_i) I\{\mathbf{X}_i \in R_{n,k}^S\} - \frac{1}{m_{n,k}} \sum_{i=1}^n g(Y_i) I\{\mathbf{X}_i \in R_{n,k}\} \right| \end{aligned} \quad (11)$$

where $0 \leq W_{n,k} \leq 1$ are weights (deterministic or random) such that $\sum_{k=1}^{K_n} W_{n,k} = 1$. In the following sections, we study the asymptotic properties of (11), breaking this up into the case of noise and signal variables.

3.1. Consistency for noise variables. The following assumptions will be used. Our first assumption requires that:

$$(A1) \quad \mathbb{E}[g(Y)^2] < \infty \text{ and } \mathbb{E}[\psi(\mathbf{X})^2] < \infty.$$

We also require ψ satisfies a smoothness property and that the features space is connected.

(A2) ψ is continuous and differentiable over the connected space $\mathcal{X} \subseteq \mathbb{R}^p$ and possesses a gradient $\mathbf{f} = \nabla\psi : \mathcal{X} \rightarrow \mathbb{R}^p$ satisfying the Lipschitz condition

$$|\mathbf{f}^{(S)}(\mathbf{x}_1) - \mathbf{f}^{(S)}(\mathbf{x}_2)| \leq C_0 |\mathbf{x}_1^{(S)} - \mathbf{x}_2^{(S)}|, \quad \text{for all } \mathbf{x}_1, \mathbf{x}_2 \in \mathcal{X}, \quad (12)$$

for some constant $C_0 < \infty$ where $\mathbf{f}^{(S)}$ denotes the subvector of \mathbf{f} with coordinates in S (note that the Lipschitz condition only applies to $\mathbf{f}^{(S)}$ as \mathbf{f} is zero over the coordinates from \mathcal{N}).

We require that regions shrink to zero uniformly over the signal features (the rate is unspecified):

(A3) For $k = 1, \dots, K_n$, $\mathbb{P}\{\mathbf{X} \in R_{n,k}\} > 0$ and $\text{diam}_S(R_{n,k}) \leq r_n$ for some sequence $r_n \rightarrow 0$ where $\text{diam}_S(R_{n,k}) = \sup_{\{\mathbf{x}_1, \mathbf{x}_2 \in R_{n,k}\}} \|\mathbf{x}_1^{(S)} - \mathbf{x}_2^{(S)}\|_2$.

The last condition pertains to the weights:

(A4) For each n , there exists $\mathbf{x}_{n,k} \in R_{n,k}$ for $k = 1, \dots, K_n$ such that

$$\sum_{k=1} W_{n,k} |\psi(\mathbf{x}_{n,k})| \leq C_1, \quad \sum_{k=1} W_{n,k} \|\mathbf{f}(\mathbf{x}_{n,k})\|_2 \leq C_2, \quad (13)$$

for some constants $C_1, C_2 < \infty$.

Assumption (A4) stipulates a trade off between the weights and the behavior of ψ and \mathbf{f} over the region of the feature space identified by a rule. Condition (13) is satisfied if ψ and \mathbf{f} are bounded. The condition also holds if all rules are constructed so their regions are contained within some closed bounded subspace in \mathcal{X} defined by the signal coordinates (because ψ and \mathbf{f} will be bounded due to continuity).

The following theorem shows that under these assumptions, VarPro is consistent for noise variables.

THEOREM 3.1. *Assume that (A1), (A2), (A3) and (A4) hold. If $K_n \leq O(\log n)$ and $m_{n,k} \geq m_n = n^{1/2} \gamma_n$ where $\gamma_n \uparrow \infty$ at a rate faster than $\log n$, then $\Delta_n(S) \xrightarrow{p} 0$ if $S \subseteq \mathcal{N}$.*

Going back to our assumptions, $\hat{\theta}_n(\zeta_{n,k}^S)$ and $\hat{\theta}_n(\zeta_{n,k})$ from (11) are averages of independent variables. Seen in this light, (A1) is really just a second moment condition needed to ensure that they converge. Assumptions (A2) and (A4) are smoothness and boundedness conditions for ψ and its derivative. Roughly speaking, since $m_n \gg n^{1/2} \rightarrow \infty$, then due to the large sample properties of averages, $\hat{\theta}_n(\zeta_{n,k}^S) - \hat{\theta}_n(\zeta_{n,k})$ converges to $\mathbb{E}(\psi(\mathbf{X})|\mathbf{X} \in R_{n,k}^S) - \mathbb{E}(\psi(\mathbf{X})|\mathbf{X} \in R_{n,k})$. For this to provide useful information about a variable's importance, it is necessary for ψ to have certain nice properties. Regarding the number of rules K_n used by the estimator, we want to use as many rules as possible to improve stability, but there is a trade-off because we also have to maintain uniform convergence, which holds when $K_n \leq O(\log n)$.

Assumption (A3) and the rate condition m_n are the only conditions that specifically apply to a region. (A3) requires that the diameter of a region shrinks to zero uniformly over the signal variables while m_n places a lower bound on the sample size of a region which must increase to ∞ . While these two conditions are diametrically opposed and therefore might seem unusual, they are fairly standard assumptions used in the asymptotic analysis of trees. For tree consistency, a typical requirement is that the diameter of a terminal node converges to 0 and the number of its points converges to ∞ in probability. See Theorem 6.1 from [13] and Theorem 4.2 from [29].

In fact, we directly show that conditions (A3) and the rate condition m_n hold for a random tree construction. Assume that $\mathcal{X} = [0, 1]^p$. Consider a tree construction where at the start of split $k \geq 1$, each of the k leaves of the tree is a p -dimensional rectangle (when $k = 1$, the one leaf equals the root node of the tree, $[0, 1]^p$). Among these k leaves (rectangles), one is selected at random and its longest side is split at a random point; yielding, at the end of step k , two new rectangles of reduced volume from the original rectangle. The tree construction is repeated for a total of K_n splits, yielding $K_n + 1$ branches which are the rules.

If $K_n = \log n$, then it can be shown that the following holds in probability [see the proof of Theorem 2 of 2]:

- (i) The number of data points in a rectangle is greater than $m_n = n^\delta \log n$ for any $1/2 < \delta < 1$.
- (ii) The mean length of the largest side of a rectangle is less than $\mathbb{E}[(3/4)^{T_n}]$ where $T_n \xrightarrow{P} \infty$ does not depend on the specific rectangle; hence the diameter of each rectangle converges uniformly to zero.

Therefore, (ii) shows (A3) holds. Also, (i) shows that $m_n \gg n^{1/2}$ achieves the lower bound required by [Theorem 3.1](#). This is an interesting consequence of the random construction and allows the bound to be achieved without supervision. This can be seen informally from the fact that $K_n = O(\log n)$ which naturally forces data to pile up in the leaves and if tree node sizes are approximately evenly distributed, $m_n \asymp n/\log n$.

3.2. Limiting behavior for signal variables. For the analysis of signal variables, we assume that regions are rectangles. This is made for technical reasons to simplify arguments but does not limit applications of VarPro. Thus, the region for a rule ζ can be written as $R(\zeta) = \times_{j=1}^p I_j$ where $I_j \subseteq \mathbb{R}$ are real-valued intervals. For notational simplicity we assume the first $|\mathcal{S}|$ coordinates are signal variables and the remaining $|\mathcal{N}|$ coordinates are noise variables. Therefore, we can write $R(\zeta) = A \times B$ where $A = \times_{j=1}^d I_j$, $B = \times_{j=d+1}^p I_j$ and $d = |\mathcal{S}| \leq p$ is the number of signal variables.

THEOREM 3.2. *Assume that the region for each rule is a rectangle contained within the connected space $X \subseteq \mathbb{R}^p$, then under the same conditions as [Theorem \(3.1\)](#), if $S = \{s\}$ is a signal variable,*

$$\Delta_n(s) = \left(1 + o_p(1)\right) \sum_{k=1}^{K_n} W_{n,k} \left| \mathbb{E} \left[\left(\psi_{n,k}^s(X^{(s)}) - \psi_{n,k}^s(x_{n,k}^{(s)}) \right) \mid \mathbf{X} \in R_{n,k}^s \right] \right| + o_p(1),$$

where $\psi_{n,k}^s(z) = \psi(x_{n,k}^{(1)}, \dots, x_{n,k}^{(s-1)}, z, x_{n,k}^{(s+1)}, \dots, x_{n,k}^{(p)})$ and $\mathbf{x}_{n,k} = (x_{n,k}^{(1)}, \dots, x_{n,k}^{(p)})' \in R_{n,k}$ is a fixed point in each rectangle as defined in (A4).

[Theorem 3.2](#) shows that the limit of the VarPro estimator is not necessarily zero as in the noise case. The limit is complicated as we would expect since it will depend on the size of the signal as well as the feature distribution, however to help understand what this limit might be, consider the case when ψ is an additive function, $\psi(\mathbf{x}) = \sum_{j=1}^d \phi_j(x^{(j)})$. Then by definition $\psi_{n,k}^s(x) = \sum_{j \in \mathcal{S} \setminus s} \phi_j(x_{n,k}^{(j)}) + \phi_s(x)$ and

$$\mathbb{E} \left[\left(\psi_{n,k}^s(X^{(s)}) - \psi_{n,k}^s(x_{n,k}^{(s)}) \right) \mid \mathbf{X} \in R_{n,k}^s \right] = \mathbb{E} \left[\left(\phi_s(X^{(s)}) - \phi_s(x_{n,k}^{(s)}) \right) \mid \mathbf{X} \in R_{n,k}^s \right]. \quad (14)$$

This is the average difference between $\phi_s(X^{(s)})$ for a random $\mathbf{X} \in R_{n,k}^s$ compared with $\phi_s(x_{n,k}^{(s)})$ for a fixed point $\mathbf{x}_{n,k} \in R_{n,k}$. Because $X^{(s)}$ is unrestricted, and can take any value in the s coordinate direction of X , $\phi_s(X^{(s)}) - \phi_s(x_{n,k}^{(s)})$ should be non-zero on average. Also, even if (14) equals zero by chance, keep in mind this applies to each rectangle $R_{n,1}, \dots, R_{n,K_n}$, thus we can expect an average nonzero effect when summing over all rules. This also explains why it is better to use many rules than just one rule. In fact, [Theorem 3.2](#) allows for up to $O(\log n)$ rules.

4. Empirical results. Here we study the performance of VarPro in regression and classification problems. [Algorithm 1](#) describes the computational procedure used for our analysis. In line 2, the data of size N is split randomly into two parts. In line 3, the first dataset of size $N - n$ is used for rule generation. In line 4, the second dataset of size n is used to obtain the importance score using the rules obtained in line 3. Data split proportions used are $0.632N$ for the rule generation step and $n = (1 - 0.632)N$ for calculating the importance score. This type of data split is fairly common in machine learning. For example, in permutation importance of random forests, each tree is constructed from a bootstrap sample of approximately $63.2\% \times N$ and the remaining $36.8\% \times N$ (the so-called out-of-bag data) is put aside for calculating permutation importance.

Algorithm 1 *VarPro for Model-Independent Variable Selection*

- 1: **for** $b = 1, \dots, B > 0$ **do**
- 2: Split the data D of size N randomly into separate parts $D = D_{\text{rg}} \cup D_{\text{vp}}$ where D_{rg} is of size $N - n$ and D_{vp} is of size $n = (1 - \alpha)N$ where $\alpha = .632$.
- 3: Use D_{rg} for the rule generation step, yielding rules $R_{n,1}, \dots, R_{n,K_n}$.
- 4: Using D_{vp} , calculate the VarPro importance (11) for variable $X^{(s)}$ for $s = 1, \dots, p$ using rules $R_{n,1}, \dots, R_{n,K_n}$ generated in the previous step. When calculating (11) use weights $W_{n,k} = m_{n,k} / \sum_{k=1}^{K_n} m_{n,k}$. Let $\Delta_n^b(s)$ denote the importance value for $s = 1, \dots, p$.
- 5: **end for**
- 6: Calculate the sample average $\bar{\Delta}_n(s)$ and sample variance $\text{Var}_n(s)$ of $\{\Delta_n^1(s), \dots, \Delta_n^B(s)\}$. Define

$$I_{n,B}(X^{(s)}) = \frac{\bar{\Delta}_n(s)}{\sqrt{\text{Var}_n(s)}}, \quad s = 1, \dots, p. \quad (15)$$

Call (15) the VarPro standardized importance of $X^{(s)}$.

We use trees for the rule generating procedure (line 3). Our trees are constructed using a guided tree-splitting strategy. As in random forests, the tree is grown using random feature selection where the split for an internal node is determined from a randomly chosen subset of features. However, instead of a uniform distribution, features are selected with probability proportional to a pre-calculated split-weight. This is done to encourage the selection of signal features in the tree construction in accordance with assumption (A3). The split-weights are obtained prior to growing the tree by taking the standardized regression coefficients from a lasso fit and adding these to the variable's split frequency obtained from a previously constructed forest of shallow trees. The rationale for this approach is that combining lasso with trees borrows the strengths of parametric and nonparametric modeling. After constructing the tree, K_n branches are randomly chosen, yielding the rules $R_{n,1}, \dots, R_{n,K_n}$ of line 3.

Finally, for the purpose of reducing variance and producing a standardized importance value, the entire procedure is repeated B times and the importance scores are standardized (line 6). Variable $X^{(s)}$ is selected if (15) exceeds a cutoff value Z_0 . This cutoff can be pre-chosen (for example $Z_0 = 2$) or selected by out-of-sample validation. Examples using both strategies will be presented.

4.1. Regression. Regression performance of VarPro was tested on 20 synthetic datasets with different N and p (see [Appendix E](#)) covering linear and nonlinear models as well as models that switched between between linear and nonlinear. Features varied from uncorrelated to correlated, with the latter retaining the same distribution but adjusted to a 0.9 correlation via a copula, except for specific cases like *lm* and *lmi2* where features were correlated within blocks of size 5 (details are provided in [Appendix E](#)).

Each VarPro run used $B = 500$ with $K_n = 75$ rules extracted. Comparison methods included permutation importance [6] (referred to as Breiman-Cutler variable importance, abbreviated as BC-VIMP), generalized boosted regression modeling (GBM) with trees; i.e. gradient boosted trees [20], knockoffs [8], lasso [63], mean decrease impurity (MDI) [51], wrappers [42] and the Relief algorithm [41] via its adaptation RReliefF [55].

R-packages used for the analysis included: `randomForestSRC` [36], `gbm` [26], `knockoff` [53], `glmnet` [18], `ranger` [68], `mlr` [4] (using a sequential forward search engine) and `CORElearn` [55]. Two types of knockoff test statistics were calculated from differences using: (1) lasso coefficient estimates and (2) random forest impurity compared to their knockoff counterparts. Two types of wrappers were used: (1) k -nearest neighbors (wrapper KNN) and (2) boosted gradient trees (wrapper GBM). The lasso regularization parameter, the number of boosting iterations for GBM and wrapper GBM and the number of nearest neighbors k for wrapper KNN were determined by 10-fold cross-validation.

Feature selection performance was assessed using the area under the precision-recall curve (AUC-PR) and the geometric mean (gmean) of TPR (true positive rate for selecting signal variables; i.e. the sensitivity) and TNR (true negative rate for selecting noise variables; i.e. the specificity). These metrics were selected since many of the simulations had far more noise variables than signal variables, presenting an imbalanced classification problem. AUC-PR evaluates the trade-off between TPR (recall) and positive predictive value (precision) without being affected by the imbalance ratio since the recall and precision are evaluated by selection thresholds varied over all possible values, making it suitable for imbalanced datasets. Gmean provides a balanced measure of performance across both the majority and minority classes, and is therefore also appropriate for class imbalanced situations [43].

To calculate AUC-PR, which does not require a threshold value, a method's output was converted to a continuous score. Scores used were: For BC-VIMP, permutation importance (a value that can be both positive and negative); for GBM, the relative influence (a non-negative value); for knockoffs, the absolute value of the knockoff test statistic; for lasso, the absolute value of the coefficient estimates; for MDI the impurity score; for ReliefF, the attribute evaluation score; for wrappers, this was a zero-one value reflecting if a variable was selected; for VarPro, the standardized importance value (15) (a non-negative value).

For gmean, a zero threshold was uniformly applied. GBM, lasso, MDI, ReliefF and wrappers used the same score value as their AUC-PR calculations. For BC-VIMP, negative importance values were converted to zero. For knockoffs, the knockoff test statistic was set to zero for variables screened under a target FDR value of 0.1. For VarPro, standardized importance was set to zero for values less than an adaptive cutoff value Z_0 selected using an out-of-sample approach. In this strategy, a grid of cutoff values is used. After ranking features in descending order of their VarPro importance, a random forest is fit to those features whose VarPro importance value is within a given cutoff value, and the out-of-bag error rate for the forest is stored. The optimized Z_0 value is defined as the cutoff with smallest out-of-bag error.

Each experiment was run 100 times independently. Results for the uncorrelated and correlated feature experiments are shown in Fig. E1 and Fig. E2 (Appendix E). We will focus on the more challenging correlated simulations. This is summarized in Fig. 3, which shows the rank of each procedure for the correlated setting. Considering Fig. E2 and Fig. 3, we can observe that BC-VIMP and GBM generally have similar behavior. Both achieve high AUC-PR values but both also have poor gmean performance. This is because while they rank variables reasonably well, which yields high AUC-PR, both methods tend to overfit and they are not able to threshold variables effectively, thus leading to a low gmean metric. The lasso and `glmnet` knockoffs show more balanced gmean results but face issues with complex models like *inx1*, *inx2*, and *inx3*, affecting their consistent performance across experiments for both

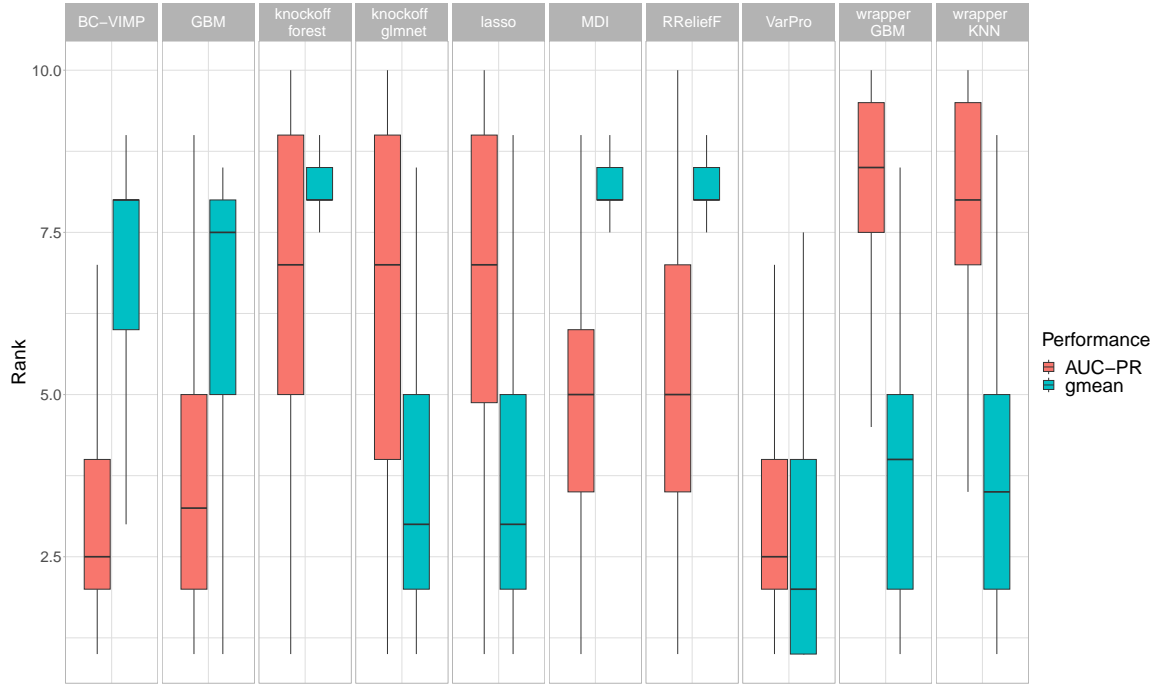


FIG 3. Rank of each procedure for correlated regression simulation experiments (lower indicates better performance).

metrics. Forest knockoffs generally underperform compared to glmnet. The KNN and GBM wrappers perform similarly and are not as effective as lasso and glmnet knockoffs. RReliefF and MDI both perform poorly in terms of gmean, with MDI slightly outperforming RReliefF in terms of AUC-PR. VarPro stands out with the best overall performance, achieving high AUC-PR for accurate variable ranking and high gmean for effective signal and noise differentiation. To test if VarPro's performance is statistically superior, we applied a paired one-sided Wilcoxon signed rank test with a Bonferroni correction for multiple comparisons. The only method equivalent to VarPro is BC-VIMP in terms of AUC-PR (adjusted p -value $<.00001$ for all other methods), and no method is equivalent or is able to outperform VarPro in terms of gmean (adjusted p -value $<.00001$). Therefore, this demonstrates VarPro has robust overall performance.

4.2. *Classification.* The following synthetic example was used to compare VarPro to random forest permutation importance. The simulation model used was a multiclass model with $L = 3$ specified according to:

$$y = \operatorname{argmax}_l \{\psi_l(\mathbf{x})\}, \quad \text{where } \psi_l(\mathbf{x}) = \frac{\phi_l(\mathbf{x})}{\sum_{l=1}^L \phi_l(\mathbf{x})}, \quad \phi_l(\mathbf{x}) = \exp\left(\sum_{j=1}^p \beta_{j,l} x^{(j)}\right)$$

$$\beta_{j,1} = 1 \text{ for } j = 1, 2, 3, \text{ otherwise } \beta_{j,1} = 0$$

$$\beta_{j,2} = 1 \text{ for } j = 4, 5, 6, \text{ otherwise } \beta_{j,2} = 0$$

$$\beta_{j,3} = 1 \text{ for } j = 7, 8, 9, \text{ otherwise } \beta_{j,3} = 0.$$

Here $X^{(1)}, \dots, X^{(9)}$ are signal variables for all three classes due to the constraint $\sum_l \psi_l = 1$. However, coordinates 1,2,3 are especially informative for class 1, coordinates 4,5,6 for class 2, and coordinates 7,8,9 for class 3. The features were drawn from a multivariate normal with marginals $X^{(j)} \sim N(0, 1)$ such that all coordinates were independent of one another, except for pairs $(X^{(3)}, X^{(10)})$, $(X^{(6)}, X^{(15)})$, $(X^{(9)}, X^{(20)})$ which were correlated with correlation $\rho = .9$. Simulations used $N = 2000$ and $p = 20$.

Standardized VarPro importance values were subtracted by the constant $Z_0 = 2$, yielding a standardized importance value for each variable $X^{(s)}$, $s \in \{1, \dots, p\}$, calibrated to zero for each class. The results from 250 independent runs are given in Fig. 4. VarPro’s results shown in the top panel are excellent which is in contrast to the bottom panel displaying permutation importance (BC-VIMP). The latter shows clear issues in separating noise from signal. The poor performance of BC-VIMP is due to the correlation between the signal variables $X^{(3)}, X^{(6)}, X^{(9)}$ and noise variables $X^{(10)}, X^{(15)}, X^{(20)}$ which causes permutation importance for signal to be degraded while artificially inflating noise importance values. In each class label instance, BC-VIMP incorrectly identifies 2 or 3 noise variables as signal. This differs from VarPro where signal variable importance is not degraded and noise importance scores are substantially smaller and all are non-significant. The group structure is also clear (for example features $X^{(1)}, X^{(2)}, X^{(3)}$ are highly informative for class 1) and it is evident that each conditional probability depends on $X^{(1)}, \dots, X^{(9)}$.

4.2.1. Low sample size, high-dimensional microarray classification experiments. In our next example we run a benchmark experiment using a collection of 22 small sample size, high-dimensional microarray datasets. The sample sizes vary from $N = 62$ to $N = 248$ and the dimensions vary from $p = 456$ to $p = 54613$. In each example the outcome is a class label where the number of classes L vary from $L = 2$ to $L = 10$. Most of the datasets are related to cancer. The data is available from the R-package `datamicroarray` and is described in more detail there.

For each dataset, the original class labels were replaced by a synthetically generated set of class labels. A parametric lasso model was fit using the original Y which was regressed using multinomial regression against \mathbf{X} equal to the gene expression values. Three different synthetic Y ’s were created. In the first, Y was the predicted class from the preliminary lasso model. In the second, the expression values were squared and then applied to the original estimated coefficients to obtain Y . The third Y was similar to the second simulation except that the top three features were replaced with their pairwise interactions. Thus we have three simulation models: (A) linear, (B) quadratic, (C) quadratic-interaction. Note that the simulated datasets use the original \mathbf{X} , only the Y is replaced with the synthetic Y and in each simulation we know which features are signal and which features are noise.

VarPro feature selection used an optimized Z_0 cutoff using out-of-sampling similar to the regression benchmark experiments. For comparison procedures, several well-known methods suitable for dealing with high-dimensional data were used: (1) BC-VIMP using the R-package `rfsrc` [36]. (2) MCFS (Monte Carlo Feature Selection) using the R-package `rmcfs` [15]. MCFS calculations were performed using the function `mcfs` where the cutoff value for thresholding was determined by permutation. As recommended by the `rmcfs` package, we used a large number of permutations and ran the MCFS algorithm for each permutation, which was used by the package to determine the permutation threshold. (3) SES (Statistically Equivalent Signature) which uses constraint-based learning of Bayesian networks for feature selection. Calculations used the `SES` function from the `MXM` R-package [46]. (4) Boruta which is a feature filtering algorithm that creates artificial data in the form of “shadow variables” which act as a reference for filtering noise variables [45]. Boruta

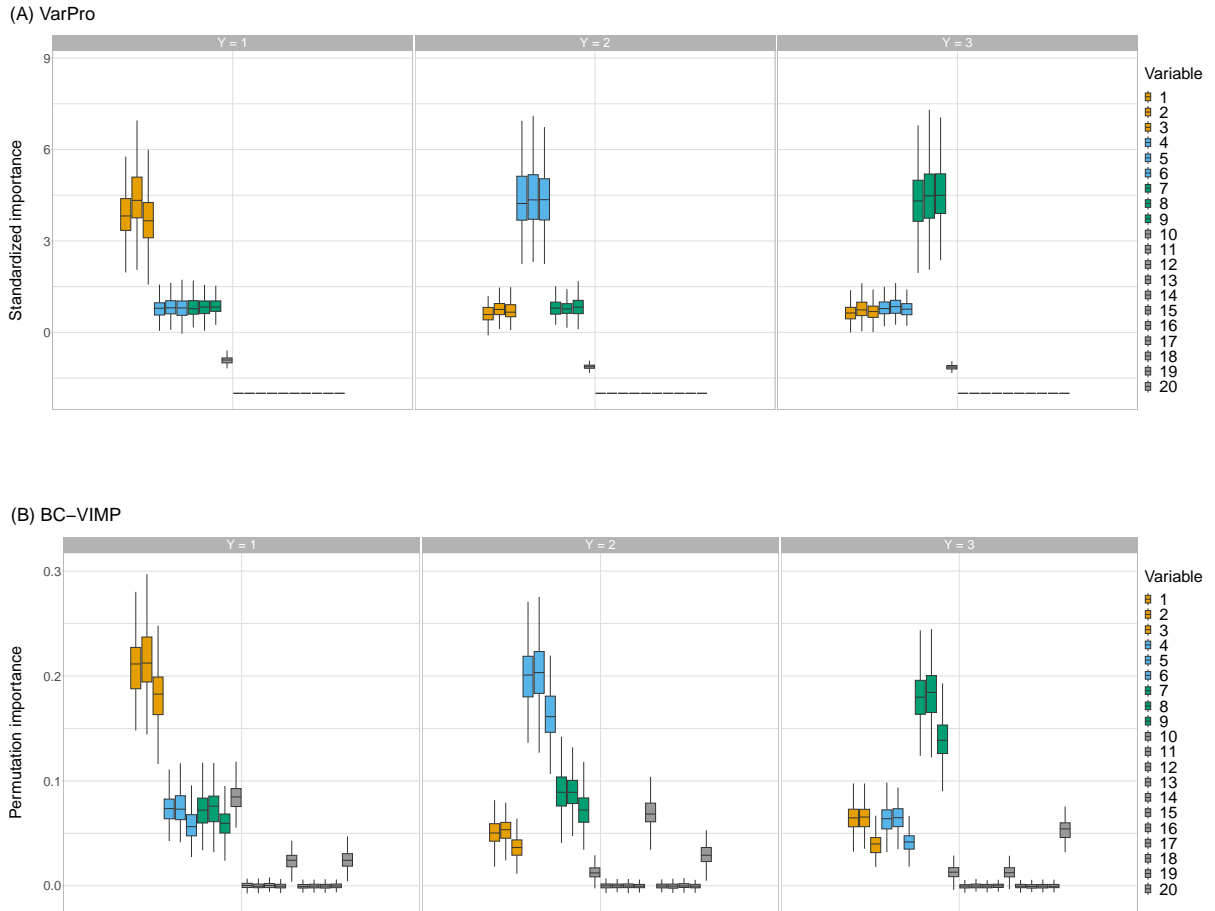


FIG 4. Multiclass experiment where variables 1–3 are most informative for class 1, variables 4–6 for class 2 and variables 7–9 for class 3; variables 10–20 are noise variables. Variables 3 and 10, 6 and 15, 9 and 20 are strongly correlated: thus there is correlation between signal and noise features. (A) VarPro importance correctly identifies the group structure and is not influenced by correlation. (B) BC-VIMP from random forests is influenced by correlation that degrades its performance.

computations were implemented using the `Boruta` R-package using random forests for the training classifier. (5) Recursive Feature Elimination (RFE) which is a wrapper feature selection procedure [28]. Calculations used the `rfe` function from the `caret` R-package [44]. Random forests were used as the RFE wrapper as recommended by [10].

The simulations were run 100 times independently for each microarray dataset. In order to introduce variability across runs, rather than using all p variables, a random subset of two-thirds of the noise variables were selected where a noise variable was defined as a gene expression feature not selected in the preliminary lasso model. Feature selection performance was assessed by geometric mean (gmean), precision (1 minus false discovery rate) and accuracy (1 minus misclassification error). Values were averaged over the 100 runs.

The results are recorded in Fig. 5. Going from scenarios (A) to (C), performance for all methods decreases as the complexity of the simulation increases as is to be expected. However, at the same time, the rank of each method and their various characteristics are maintained across simulations. BC-VIMP is always one of the best procedures in terms of gmean whereas it is always one of the worst for precision and accuracy. SES is always the worst

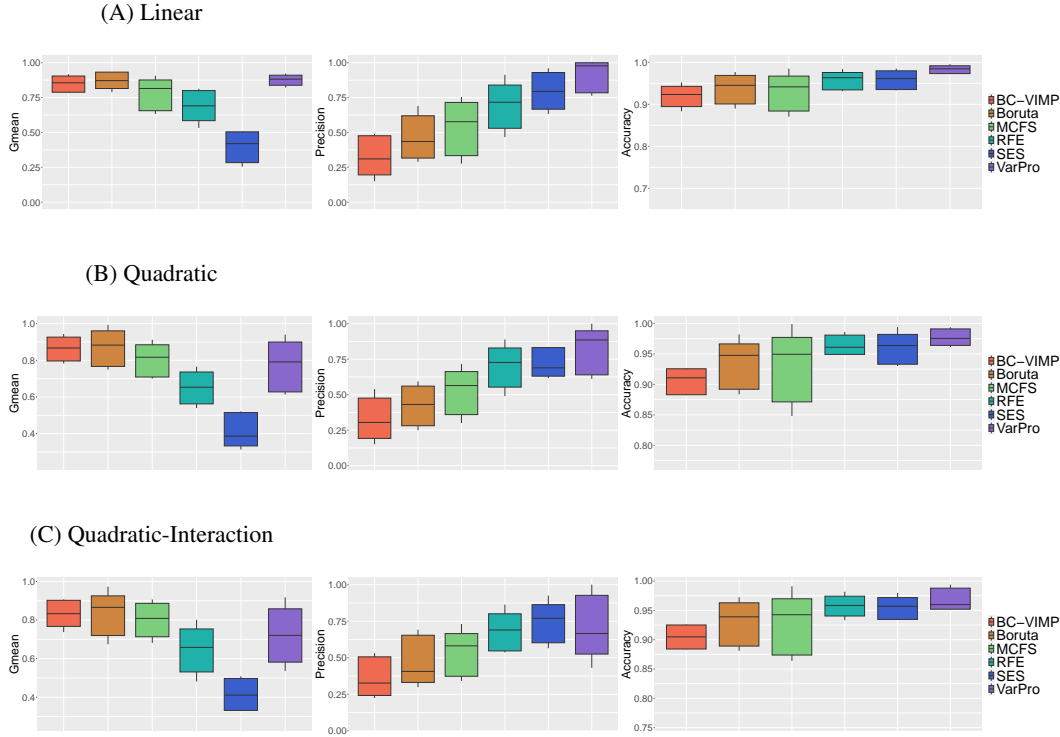


FIG 5. Feature selection performance over high-dimensional microarray classification datasets. Three simulation models were used for creating synthetic Y classification labels: (A) Linear; (B) Quadratic; (C) Quadratic-Interaction.

in terms of gmean performance, but it is always among the top performers for precision and accuracy. VarPro, on the other hand, does well in all three metrics and has better overall performance than any other method (adjusted p -value < 0.05 for all experiments). These results are consistent with our benchmark regression experiments that showed VarPro achieves a balanced performance.

4.2.2. *DNA methylation subtypes for adult glioma multiclassification.* In our next example we reanalyze a subset of data used by [9] for studying adult diffuse gliomas. The study used DNA methylation data obtained from CpG probes for molecular profiling. A total of $p = 1206$ probes collected over $N = 880$ human tissues was used in their analysis.

An important finding in [9] was that DNA methylation was effective in separating glioma subtypes. To informally validate these results, we use the clusters developed in the study as outcomes in a multiclass analysis. There were $L = 7$ labels: Classic-like, Codel, G-CIMP-high, G-CIMP-low, LGm6-GBM, Mesenchymal-like, and PA-like. For an added challenge, clinical data and molecular data available for the samples were also included as features for the VarPro analysis. In total, $p = 1241$ variables were used. The data is available from the R-package `TCGAbiolinksGUI.data` [57].

Fig. 6 displays the VarPro standardized importance values for the selected features. IDH status, telomere length, and TERT promoter status, which were three of the added molecular variables, are seen to be informative. [9] found that IDH status was a major determinant of the molecular profile of diffuse glioma, so these results are in agreement with the original study. The VarPro analysis also identified DNA methylation probes with significant impor-

tance values. This is interesting and useful since it identifies probes that potentially provide additional power to separate subtypes beyond the molecular variables mentioned.

To explore the ability of probes to separate subtypes, Fig. 7 shows some of the top DNA methylation probes versus glioma subtypes. Data distribution for each variable and frequency distribution of cluster subtype is given along the diagonal. Lower subdiagonal blocks in blue are scatter plots of probe values in pairs; upper subdiagonal in purple are density contours for the pairs. Boxplots in red show DNA methylation probe values for each subtype. For example, the top right boxplot is cg15439862, which shows particularly low values for LGM6-GBM and Mesenchymal compared to other subtypes, indicating this probe's effectiveness in distinguishing these two subtypes from the rest. Similar patterns are observed with other probes, demonstrating their ability to separate subtypes. These results support the conclusions of the original study and highlight VarPro's effectiveness in addressing high-dimensional bioinformatic challenges.

5. Modified VarPro using external estimators: time to event data. Now we discuss the use of external estimators, which is a way to extend the VarPro method from being model-independent to model-specific. Recall that VarPro estimates $\psi(\mathbf{X}) = \mathbb{E}(g(Y) | \mathbf{X})$ by using a sample average of $g(Y)$ calculated locally within a region defined by a rule. For a rule $\zeta_{n,k}$ and its region $R_{n,k} = R(\zeta_{n,k})$ with sample size $m_{n,k}$, VarPro makes use of the estimator (4)

$$\hat{\theta}_n(\zeta_{n,k}) = \frac{1}{m_{n,k}} \sum_{i=1}^n g(Y_i) I\{\mathbf{X}_i \in R(\zeta_{n,k})\}.$$

However, depending on the complexity of the problem, this may not always be suitable as it could be inefficient or difficult to estimate ψ locally this way.

The strategy to overcome this is to use an external estimator building on the ideas discussed in Section 2. For each n , let $\psi_n : \mathcal{X} \rightarrow \mathbb{R}$ be an external estimator for ψ . The modified VarPro estimator is defined as follows. For each rule $\zeta_{n,k}$, the modified procedure replaces $\hat{\theta}_n(\zeta_{n,k})$ with

$$\tilde{\theta}_n(\zeta_{n,k}) = \frac{1}{m_{n,k}} \sum_{i=1}^n \psi_n(\mathbf{X}_i) I\{\mathbf{X}_i \in R_{n,k}\}.$$

Likewise, the release rule $\hat{\theta}_n(\zeta_{n,k}^S)$, which releases the rule $\zeta_{n,k}$ along the coordinates of a set $S \subset \{1, \dots, p\}$, is replaced with

$$\tilde{\theta}_n(\zeta_{n,k}^S) = \frac{1}{m_{n,k}^S} \sum_{i=1}^n \psi_n(\mathbf{X}_i) I\{\mathbf{X}_i \in R_{n,k}^S\}.$$

Therefore, $g(Y_i)$ used in the original formulation is replaced with $\psi_n(\mathbf{X}_i)$ which serves to estimate the conditional mean of $g(Y_i)$. Given rules $\zeta_{n,1}, \dots, \zeta_{n,K_n}$, the modified VarPro measure of importance for S is

$$\tilde{\Delta}_n(S) = \sum_{k=1}^{K_n} W_{n,k} |\tilde{\theta}_n(\zeta_{n,k}^S) - \tilde{\theta}_n(\zeta_{n,k})|$$

for prechosen weights $0 \leq W_{n,k} \leq 1$, $\sum_{k=1}^{K_n} W_{n,k} = 1$.

An important application of the modified procedure is survival analysis. This is because trying to locally estimate the survival function is difficult if right censoring is present. In such settings, due to censoring, the observed data is (T, δ, \mathbf{X}) , where $T = \min(T^o, C^o)$ is the time of event, $\delta = I\{T^o \leq C^o\}$ is the censoring indicator, and T^o, C^o are the true survival

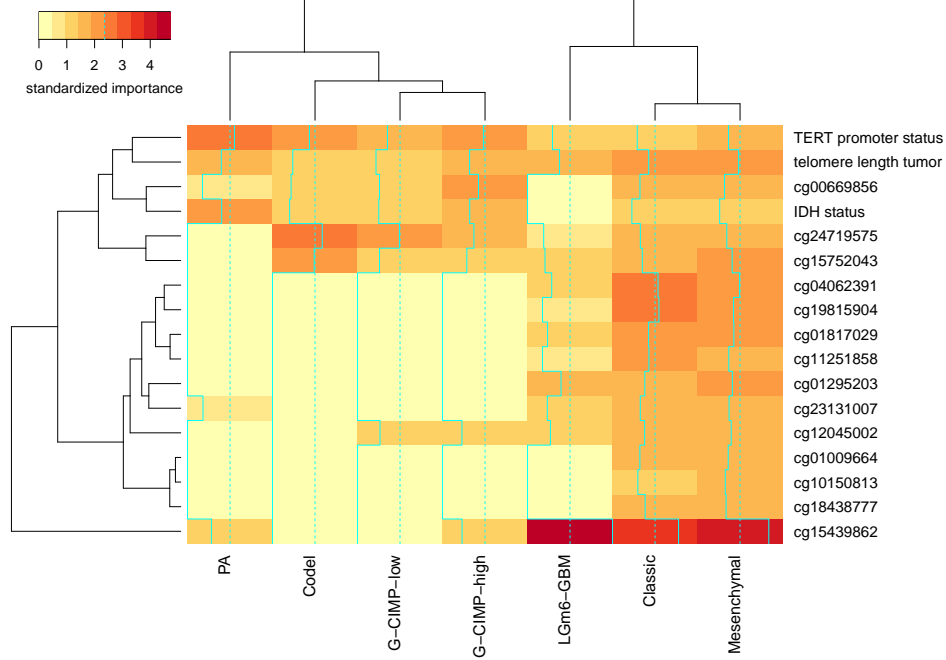


FIG 6. Heatmap of standardized importance from VarPro multiclass analysis of adult glioma DNA methylation data ($N = 880$, $p = 1241$).

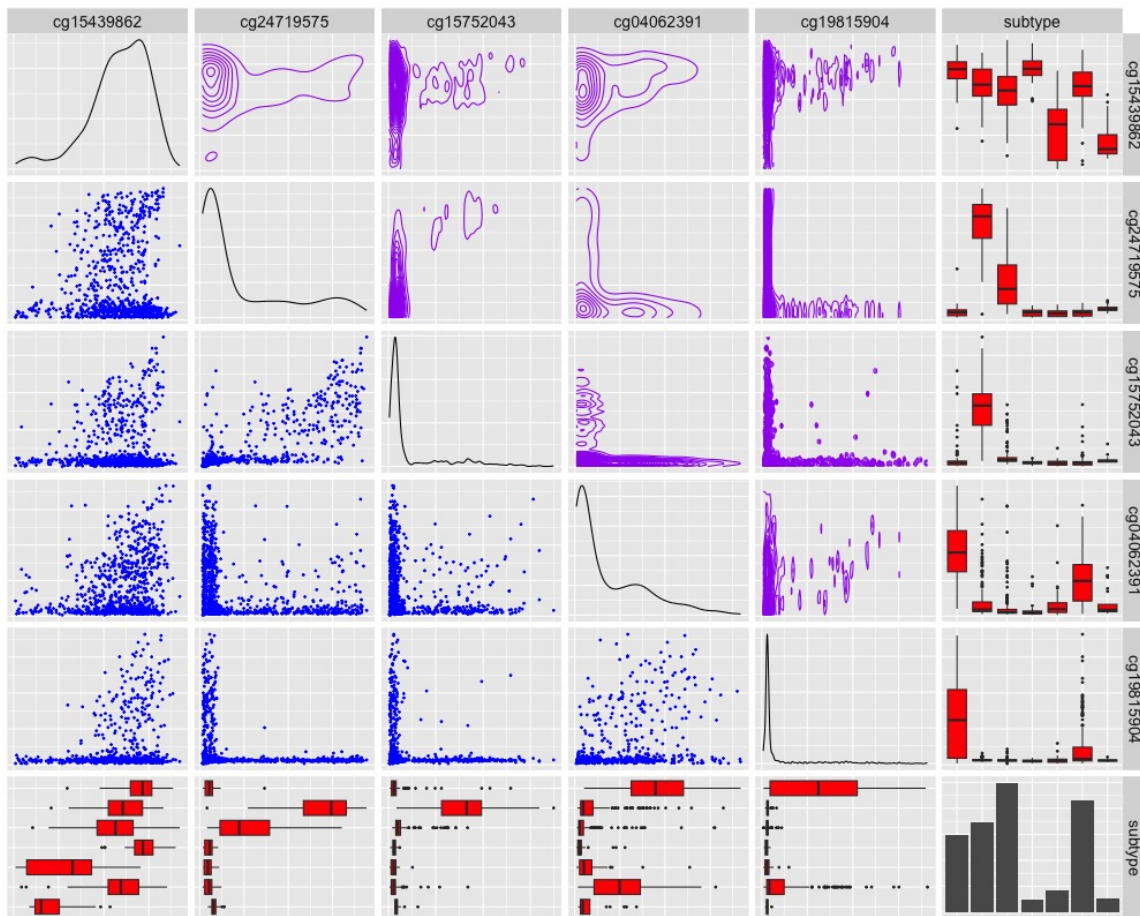


FIG 7. DNA methylation probe values and glioma subtypes.

and censoring times. Because only $(\min(T^o, C^o), \delta, \mathbf{X})$ is observed, the time of event is only observed if censoring is not present. The survival function is $S(t | \mathbf{X}) = \mathbb{P}\{T^o > t | \mathbf{X}\}$, and this corresponds to $\psi(\mathbf{X}) = \mathbb{E}(g(T^o) | \mathbf{X})$ where $g(T^o) = I\{T^o > t\}$. Let ζ be a rule and $R(\zeta)$ its region. Because T^o is potentially unobserved, we cannot estimate $S(t | \mathbf{X})$ locally using an estimator like

$$\hat{\theta}_n(\zeta) := \frac{\sum_{i=1}^n g(Y_i) 1_{\{\mathbf{X}_i \in R(\zeta)\}}}{\sum_{i=1}^n I\{\mathbf{X}_i \in R(\zeta)\}} = \frac{\sum_{i=1}^n I\{T_i^o > t, \mathbf{X}_i \in R(\zeta)\}}{\sum_{i=1}^n I\{\mathbf{X}_i \in R(\zeta)\}}.$$

If we want to use a sample average of the observed data, as in the original VarPro formulation, then we have to account for censoring. For example, under the assumption of conditional independence, one approach could be to use an IPCW (inverse of probability of censoring weighting) estimator such as

$$\hat{\theta}_n(\zeta) = \left(\sum_{i=1}^n I\{\mathbf{X}_i \in R(\zeta)\} \right)^{-1} \sum_{i=1}^n \frac{\delta_i}{G(T_i)} \left[I\{T_i > t, \mathbf{X}_i \in R(\zeta)\} \right]$$

where $G(u) = \mathbb{P}\{C > u\}$ is the unknown censoring distribution. However, there are known issues with IPCW estimators, such as estimation for G , and problems with inverse weights becoming large [25, 24].

As another example, consider variable selection for the restricted mean survival time (RMST) [33, 1, 56, 40]. The RMST is a useful quantity summarizing lifetime behavior and is defined as the survival function integrated from $[0, \tau]$

$$\int_0^\tau S(t | \mathbf{X}) dt = \mathbb{E} \left[\int_0^\tau 1_{\{T^o > t\}} dt | \mathbf{X} \right] = \mathbb{E} \left[\int_0^{T^o \wedge \tau} dt | \mathbf{X} \right] = \mathbb{E} [T^o \wedge \tau | \mathbf{X}]. \quad (16)$$

The time horizon τ is usually selected to represent a clinically meaningful endpoint, such as 1 year or 5 year survival. Just like the survival function due to censoring, the RMST is difficult to estimate locally. Therefore, using an external estimator is a way to overcome this issue.

The following result shows that the modified VarPro procedure is consistent under the assumption (A5) that ψ_n converges uniformly to ψ . While this might seem to be a strong assumption, convergence only has to hold over a suitably defined subspace (see Appendix F for further discussion regarding (A5)).

THEOREM 5.1. *The conclusions of Theorem 3.1 and Theorem 3.2 hold for $\tilde{\Delta}_n(S)$ under their stated conditions if in addition assumption (A5) of Appendix F holds.*

In the next subsections we present examples illustrating the modified procedure applied to right censored survival settings.

5.1. High-dimensional, low sample size, variable selection for survival. For our first illustration we consider a high-dimensional survival simulation. The survival time T^o was simulated by

$$T^o = \log \left[1 + V \exp \left(\sum_{j=1}^p \beta_j \{X^{(j)}\}^2 \right) \right], \quad V \sim \frac{4}{10} \exp(.5) + \frac{1}{10} \exp(1) + \frac{2}{10} \exp(1.5) + \frac{3}{10} \exp(3)$$

where V was sampled independently of \mathbf{X} and is a four-component mixture of exponential random variables with rate parameters (inverse means) .5, 1, 1.5, 3. The first $p_0 = 10$ features of \mathbf{X} were signal variables: these were assigned coefficient values $\beta_j = \frac{1}{2} \log(1 + \sqrt{p/p_0})$.

All features had marginal uniform $U(0, 1)$ distributions. The noise features were uncorrelated; the signal features had pairwise correlation $\rho = 3/7$. Random censoring at 50% and 75% rates were used. A sample size $N = 200$ was used while varying p .

For ψ , we used the integrated cumulative hazard function (CHF) and for the external estimator ψ_n , we chose random survival forests (RSF) [37] using the `randomForestSRC` package [36]. Because the ensemble CHF is piecewise constant, no approximation was needed to integrate it.

Comparison procedures included Cox regression with lasso penalization (`coxnet`) using the `glmnet` package [58] and BC-VIMP and minimal depth (MD) [39, 38] using the `randomForestSRC` [36] R-package. These methods were specifically selected due to their proven effectiveness in feature selection for high-dimensional survival problems. Given the complex nature of the simulations, careful tuning was necessary for all methods. For `coxnet`, the default one-standard error rule from `glmnet` for choosing the lasso regularization parameter λ during 10-fold validation resulted in overly sparse solutions. Therefore, we opted for the λ that produced the smallest out-of-sample error (the minimum rule). For minimal depth, we used the mean minimal depth threshold value [39, 38]. For VarPro, the Z_0 cutoff value was obtained using an out-of-sample technique similar to the regression and classification benchmark experiments of Section 4. Specifically, sequential models used to select the optimized cutoff value were fit using RSF. Out-of-sample performance was evaluated using the continuous rank probability score (CRPS) [25, 23].

Simulations were repeated 100 times independently. Feature selection was assessed by `gmean`, precision and accuracy. The results were averaged across the runs and are given in Table 1. Similar to our previous benchmark experiments for regression and classification, we observe that VarPro achieves the best overall performance in all metrics (adjusted p -value < 0.00001)

TABLE 1

High-dimensional survival simulation ($N = 200$, $p = 500, 1000, 1500$ and $p_0 = 10$) where signal variables are correlated. Random censoring was applied at 50% and 75% rates. Results are averaged over 100 independent runs.

	p	50% Censoring			75% Censoring		
		Gmean	Precision	Accuracy	Gmean	Precision	Accuracy
coxnet	500	0.91	0.49	0.97	0.77	0.42	0.97
	1000	0.93	0.42	0.98	0.79	0.36	0.98
	1500	0.94	0.39	0.99	0.79	0.32	0.99
VarPro	500	0.95	0.55	0.98	0.87	0.42	0.97
	1000	0.96	0.53	0.99	0.91	0.43	0.99
	1500	0.97	0.57	0.99	0.92	0.43	0.99
BC-VIMP	500	0.86	0.07	0.74	0.81	0.06	0.70
	1000	0.89	0.05	0.79	0.84	0.04	0.75
	1500	0.91	0.04	0.82	0.86	0.03	0.79
MD	500	0.88	0.37	0.80	0.77	0.41	0.81
	1000	0.88	0.43	0.82	0.72	0.38	0.79
	1500	0.89	0.52	0.84	0.67	0.52	0.83

5.2. *Heart rate recovery long term survival.* Exercise stress testing is commonly used to assess patients with known or suspected coronary artery disease. A useful predictor of mortality is fall in heart rate immediately after exercise stress testing, or heart rate recovery [32]. Heart rate recovery is defined as the heart rate at peak exercise minus the heart rate measured

1 minute later. The hypothesis that heart rate recovery predicts mortality has been tested and validated in a number of cohorts [12]. Here we study this issue by considering how predictive heart rate recovery is in the presence of other potentially useful features by making use of the modified VarPro procedure.

For this analysis we use data from the study in [35]. The study considered $N = 23,701$ patients referred for symptom-limited exercise testing. Each patient underwent an upright cool-down period for the first 2 minutes after recovery. Detailed data regarding reason for testing, symptoms, cardiac risk factors, other medical diagnoses, prior cardiac and noncardiac procedures, medications, resting electrocardiogram, resting heart rate, and blood pressure were recorded prospectively prior to testing. During each stage of exercise, and during the first 5 minutes of recovery, data were recorded regarding heart rate, blood pressure, ST-segment changes, symptoms, and arrhythmias. In total $p = 85$ variables were available for the analysis. All cause mortality was used for the survival outcome. Data was right-censored with mean follow-up of 5.7 years (range .75 to 10.1 years) during which 1,617 patients died.

For ψ , we use the RMST evaluated at $\tau = 3$ years. The RMST was calculated by (16) using the estimated survival function from a RSF analysis. As before, calculations used the `randomForestSRC` package [36]. The standardized importance values from VarPro are given in Fig. 8 (D). Signal variables (red) and noise variables (blue) are identified using a Z_0 cutoff value where the latter was calculated using an out-of-sample strategy as in the previous section. From the figure, we can observe that heart rate recovery is identified as a signal variable. However, at the same time, we also observe several other significant variables, some with even larger importance values, such as age, peak met, peak heart rate and sex.

For comparison, we re-analyzed the data using tree boosting with Cox regression. Computations were run using the R-package `gbm` [26]. The top 5 variables from boosting were age, peak met, heart rate recovery, COPD and heart rate, which generally agree with the top variables found by VarPro. However, an interesting difference between the two procedures was their ranking for sex. VarPro ranked sex as among its top 5 variables whereas sex did not even make it into the top 12 variables for boosting. This is important because sex is a variable that is often overlooked in the heart failure literature.

Further analysis is presented with separate Kaplan-Meier survival curves for men and women in Fig. 8 (A), showing minimal differences. However, when stratifying peak met (a significant variable) into deciles and plotting survival curves for each category, a notable distinction emerges. For men (C), survival decreases more significantly than for women (B) at lower peak met values (survival curves descending from top to bottom). This suggests that men are more adversely affected by reduced peak met, implying greater sensitivity to exercise capacity, as peak met is an indicator of this. These observations are consistent with prior research by [31], which indicated that women have a lower mortality risk than men at any given level of exercise or oxygen capacity.

6. Discussion. We demonstrated that VarPro performs well in many settings. In a large cardiovascular survival study (Section 5), VarPro was able to identify a variable without a main effect but with a strong interaction, which led to discovering a meaningful difference in long-term survival for patients at risk for heart disease. This is impressive because identifying variables with no main effects but significant interactions is generally considered difficult, even for the very best variable selection methods. The ability to deal with interactions was also evident in the synthetic regression experiments (Section 4), where models frequently included interaction terms. VarPro not only performed well but also stood out in scenarios with correlated features, which is valuable since real-world data often involves complex interactions and correlations. Section 4 provided further illustration of the ability to handle real-world correlation using a large benchmark analysis of microarray datasets.

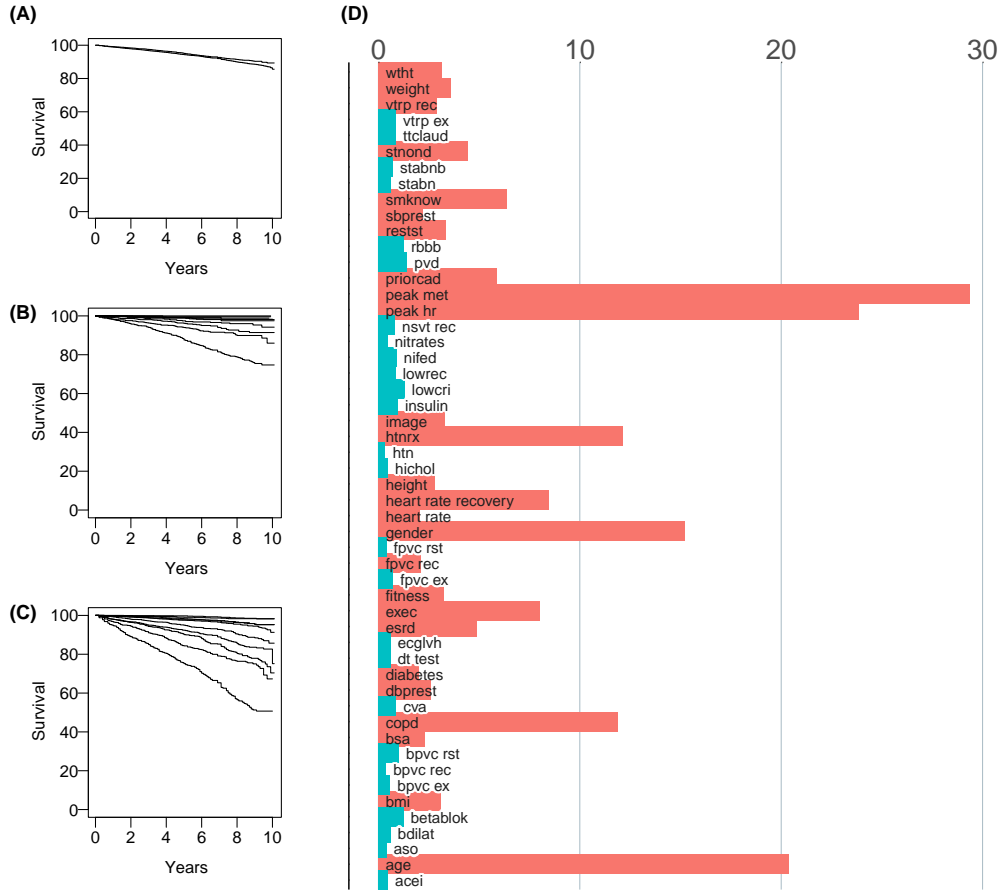


FIG 8. Results of heart rate recovery survival analysis using the modified VarPro procedure. (A) Survival for men and women; (B) Survival for women, stratified by peak met; (C) Survival for men, stratified by peak met; (D) Standardized importance for variables (red are signal, blue are noise variables).

Another strength of VarPro is that it makes use of rule-based selection. This replaces the problem of building a high-performance model [49, 47] with a series of lower-dimensional localized variable selection problems that can be solved computationally fast. All the examples presented in this paper can be computed efficiently, and in our experience, we have found VarPro to be very fast. As an illustration, Fig. 9 shows the CPU times for VarPro (red lines) across different simulation sizes from $N = 250$ to $N = 15,000$ and dimensions from $p = 10$ to $p = 5000$ using the Friedman 1 regression simulation (Appendix E). For context, CPU times for BC-VIMP (black lines) using the R-package ranger [68] and for gradient boosting (blue lines) using the R-package gbm [26] are also displayed, noting that gradient boosting times were limited by sample sizes and dimensions due to long run time durations. VarPro’s run times prove to be more favorable as N and p increase, highlighting its computational efficiency and viability in handling large datasets compared to existing methods.

Despite the encouraging results, the method can still be enhanced. A potential area for improvement is rule generation. Our approach utilized trees guided by split-weights derived from combining lasso with shallow trees. Although effective in this context, the development of automated strategies for generating high-performing rules needs additional exploration. Nonetheless, a strength of our methodology lies in providing a theoretical road map for what

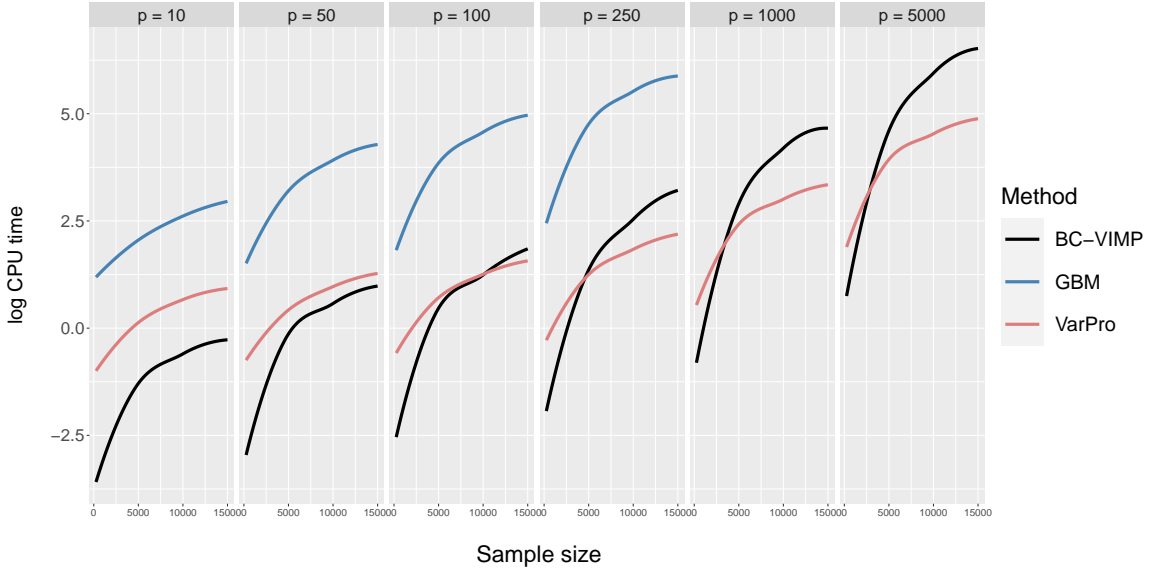


FIG 9. Log CPU times in seconds for VarPro (red lines) using the Friedman 1 simulation (Appendix E) with varying sample size N and dimension p . Shown for comparison are log CPU times for BC-VIMP (black lines) using the *ranger* R-package (500 trees used for each forest) and gradient boosting (blue lines) using the *gbm* R-package (the optimal number of trees used in each boosted experiment was determined by 10-fold validation with a maximum value of 2000 trees).

needs to be done. The rule generation step needs to guarantee that regions for signal variables shrink to zero, but as has been pointed out, such an assumption seems reasonable. Given the minimal assumptions on rule construction, this approach should facilitate further adaptations and applications.

Another potential limitation is identification of signal variables in scenarios where a unique Markov boundary may not exist. As discussed by [59], there can be multiple Markov boundaries of the response variable. In other words, ψ may not be identified because several variables could interchangeably provide the same amount of information for ψ . Since our current discovery algorithm is to quantify the relative importance of predictors one by one, we tend to select the signal variables as the union set of multiple Markov boundaries that contain redundant information. However, in this case, our method retains its property of being able to filter noise variables.

We use the following simulation for illustration. Data was drawn from the regression model

$$Y = X^{(1)} + X^{(2)} + \varepsilon, \quad \varepsilon \sim \mathbf{N}(0, 1).$$

The feature vector is of dimension $p = 150$ and drawn from a multivariate normal with zero mean and equicorrelation matrix with correlation parameter $\rho = .4$. Variables $X^{(3)}$ and $X^{(4)}$ were modified so that

$$X^{(3)} = \beta X^{(1)} + (1 - \beta)X^{(2)}, \quad X^{(4)} = (1 - \beta)X^{(1)} + \beta X^{(2)}.$$

Therefore, this reflects a regression setting where some columns are linearly related to others. Notice that

$$\psi(\mathbf{X}) = \mathbb{E}(Y|\mathbf{X}) = X^{(1)} + X^{(2)} = X^{(3)} + X^{(4)}.$$

Therefore according to [Definition 1.1](#), the signal variables must be $\mathcal{S} = \{1, 2, 3, 4\}$. It cannot be $\mathcal{S} = \{1, 2\}$, since we would have $\psi(\mathbf{X}) = \psi(\mathbf{X}^{\setminus\{3,4\}}) = \psi(\mathbf{X}^{\{3,4\}})$. Likewise it cannot be $\mathcal{S} = \{3, 4\}$, since then $\psi(\mathbf{X}) = \psi(\mathbf{X}^{\setminus\{1,2\}}) = \psi(\mathbf{X}^{\{1,2\}})$. Therefore \mathcal{S} must contain all 4 variables, creating a redundant scenario.

For demonstration, VarPro was executed 1000 times independently using the above simulation, with a sample size of $N=1500$ and $\beta = 1/4$. The first row of [Table 2](#) lists the averaged standardized importance for the first 4 variables, while all remaining variables are grouped under the “noise” category. The second row shows the frequency of each variable’s selection. The results highlight VarPro’s capabilities: (1) efficiently weeding out noise variables and (2) identifying redundant signal variables, confirming the earlier statements about VarPro’s performance in scenarios with non-unique Markov boundaries.

TABLE 2

Regression simulation with non-unique Markov boundary. The first row lists VarPro standardized importance values. The second row lists the selection frequency for each variable. The conditional mean can be described by both $\{X^{(1)}, X^{(2)}\}$ and $\{X^{(3)}, X^{(4)}\}$, therefore there is redundancy in the definition of a signal variable. Variables $X^{(j)}$ for $j = 5, \dots, 150$ are combined into category “noise”.

	$X^{(1)}$	$X^{(2)}$	$X^{(3)}$	$X^{(4)}$	noise
Importance	5.63	5.61	10.30	10.29	0.00
Percent	98.70	99.10	100.00	100.00	0.03

APPENDIX A: UNIFORM APPROXIMATION FOR THE AVERAGE SIZE OF A REGION

The following lemma will be used in several places and provides a uniform approximation for the average sample size of a region. The notation $b_n \gg a_n$ is used to signify $b_n/a_n \rightarrow \infty$.

LEMMA A.1. *Let $R_{n,k} \subseteq \mathcal{X}$ be a collection of sets such that $\mathbb{P}\{R_{n,k}\} > 0$, $k = 1, \dots, K_n$, and define $m_{n,k} = \sum_{i=1}^n I\{\mathbf{X}_i \in R_{n,k}\}$ where $\mathbf{X}_1, \dots, \mathbf{X}_n$ are i.i.d. random vectors over \mathcal{X} . If $K_n \leq O(\log n)$ and $m_{n,k} \geq m_n \gg \sqrt{n \log \log n}$, then the following identity holds over a set with probability tending to one uniformly over $k = 1, \dots, K_n$:*

$$\frac{n}{m_{n,k}} = \frac{1}{\mathbb{P}(R_{n,k})} \left(1 + \xi_{n,k}^*\right), \quad \text{where } |\xi_{n,k}^*| \leq \frac{\sqrt{\log \log n}}{n^{-1/2} m_n} \rightarrow 0. \quad (17)$$

PROOF. Observe that $m_{n,k} = \sum_{i=1}^n I\{\mathbf{X}_i \in R_{n,k}\}$ is a sum of i.i.d. Bernoulli random variables. Therefore by Hoeffding’s inequality [\[30\]](#),

$$\mathbb{P} \left\{ \max_{1 \leq k \leq K_n} |n^{-1} m_{n,k} - \mathbb{P}(R_{n,k})| \geq \varepsilon \right\} \leq 2K_n \exp(-2\varepsilon^2 n).$$

Let \mathcal{A}_n^c be the event inside the probability. If ε is allowed to depend on n so that $2\varepsilon^2 n \geq 2(\log \log n)$, then the bound on the right is order $K_n (\log n)^{-2} \rightarrow 0$. Therefore over \mathcal{A}_n , an event which occurs with probability tending to one,

$$|\xi_{n,k}^*| \leq \xi_n, \quad \text{where } \xi_{n,k} = \mathbb{P}(R_{n,k}) - n^{-1} m_{n,k}, \quad \xi_n = n^{-1/2} \sqrt{\log \log n}.$$

Using $m_{n,k} \geq m_n$, then with probability tending to one over \mathcal{A}_n :

$$\frac{n}{m_{n,k}} = \frac{1}{\mathbb{P}(R_{n,k})} + \frac{\xi_{n,k}^*}{\mathbb{P}(R_{n,k})}, \quad \text{where } \left| \xi_{n,k}^* := \frac{\xi_{n,k}}{n^{-1} m_{n,k}} \right| \leq \frac{\xi_n}{n^{-1} m_n}.$$

Upon rearrangement this gives [\(17\)](#). □

APPENDIX B: UNIFORM APPROXIMATION FOR SAMPLE AVERAGES WITH
VARYING SIZE

In order for $\Delta_n(S)$ to have good theoretical performance, $\hat{\theta}_n(\zeta_{n,1}), \dots, \hat{\theta}_n(\zeta_{n,K_n})$ and the released values $\hat{\theta}_n(\zeta_{n,1}^S), \dots, \hat{\theta}_n(\zeta_{n,K_n}^S)$ must be controlled uniformly. This imposes a limit on the sequences $K_n, m_n(\zeta_{n,k})$ and $m_n(\zeta_{n,k}^S)$. We describe a lemma for this purpose.

First we rewrite the VarPro estimators in a slightly different way. For a given rule ζ , let $b(\zeta) = \mathbb{E}[\psi(\mathbf{X})I\{\mathbf{X} \in R(\zeta)\}]$ where recall that $\psi(\mathbf{X}) = \mathbb{E}(g(Y)|\mathbf{X})$. Notice that $\hat{\theta}_n$ can be rewritten as

$$\hat{\theta}_n(\zeta) = \frac{1}{m_n(\zeta)} \sum_{i=1}^n Z_i(\zeta) + \frac{nb(\zeta)}{m_n(\zeta)}, \quad (18)$$

where $Z_i(\zeta) = g(Y_i)I\{\mathbf{X}_i \in R(\zeta)\} - b(\zeta)$ are i.i.d. random variables with a mean of zero:

$$\begin{aligned} \mathbb{E}(Z_i(\zeta)) &= \mathbb{E}\left\{ \mathbb{E}\left[(g(Y) - \psi(\mathbf{X}))I\{\mathbf{X} \in R(\zeta)\} \mid \mathbf{X} \right] \right\} \\ &= \mathbb{E}\left\{ I\{\mathbf{X} \in R(\zeta)\} \mathbb{E}\left[(g(Y) - \psi(\mathbf{X})) \mid \mathbf{X} \right] \right\} = 0. \end{aligned}$$

Recall that $m_{n,k} = m_n(\zeta_{n,k})$, $m_{n,k}^S = m_n(\zeta_{n,k}^S)$ and $R_{n,k} = R(\zeta_{n,k})$, $R_{n,k}^S = R(\zeta_{n,k}^S)$. Applying a similar centering as in (18) to the released rule, we have

$$\begin{aligned} \hat{\theta}_n(\zeta_{n,k}^S) - \hat{\theta}_n(\zeta_{n,k}) &= \left[\frac{1}{m_{n,k}^S} \sum_{i=1}^n Z_i(\zeta_{n,k}^S) - \frac{1}{m_{n,k}} \sum_{i=1}^n Z_i(\zeta_{n,k}) \right] \\ &\quad + \left[\frac{nb(\zeta_{n,k}^S)}{m_{n,k}^S} - \frac{nb(\zeta_{n,k})}{m_{n,k}} \right], \end{aligned} \quad (19)$$

where (similar definitions apply to $\zeta_{n,k}^S$):

$$Z_i(\zeta_{n,k}) = g(Y_i)I\{\mathbf{X}_i \in R_{n,k}\} - b(\zeta_{n,k}), \quad b(\zeta_{n,k}) = \mathbb{E}[\psi(\mathbf{X})I\{\mathbf{X} \in R_{n,k}\}].$$

The sums appearing in (19) will be shown to converge to zero uniformly using the lemma given next. The quantity in the second square bracket will be dealt with later. It represents a ‘‘bias’’ term that is asymptotically zero for noise variables but non-zero for signal variables.

B.1. Key lemma for uniform approximation of sample averages. For each n , let $Z_{1,k}^{(n)}, \dots, Z_{n,k}^{(n)}$ be independent random variables such that $\mathbb{E}(Z_{i,k}^{(n)}) = 0$ and $\mathbb{E}[(Z_{i,k}^{(n)})^2] \leq \sigma^2 < \infty$ for $i = 1, \dots, n$ and $k = 1, \dots, K_n$. Let

$$S_{n,k} = \sum_{i=1}^n Z_{i,k}^{(n)}, \quad \text{and} \quad T_{n,k} = \frac{1}{M_{n,k}} \sum_{i=1}^n Z_{i,k}^{(n)} = \frac{1}{M_{n,k}} S_{n,k}$$

where $M_{n,k}$ are random values (not necessarily independent of $Z_{1,k}^{(n)}, \dots, Z_{n,k}^{(n)}$) satisfying $n \geq M_{n,k} \geq M_n > 0$ for $k = 1, \dots, K_n$. We wish to identify conditions for the deterministic sequences M_n, K_n such that $T_{n,k}$ converges to zero uniformly over $k = 1, \dots, K_n$ as $n \rightarrow \infty$.

Let $L_n = (nK_n)^{-1/2}$. Then by Chebyshev’s inequality, for any constant $C > 0$,

$$\mathbb{P}\{L_n |S_{n,k}| \geq C\} = \mathbb{P}\left\{ \left| \sum_{i=1}^n Z_{i,k}^{(n)} \right| \geq \frac{C}{L_n} \right\} \leq \frac{L_n^2}{C^2} \sum_{i=1}^n \mathbb{E}[(Z_{i,k}^{(n)})^2] \leq \frac{\sigma^2}{C^2 K_n}. \quad (20)$$

Let $\mathcal{B}_{n,k} = \{\omega : |L_n S_{n,k}| \geq C\}$ and $\mathcal{B}_n = \bigcup_{k=1}^{K_n} \mathcal{B}_{n,k}$. Because $M_{n,k} \geq M_n$, setting $\delta_n = L_n^{-1} M_n^{-1} = M_n^{-1} (nK_n)^{1/2}$ we obtain

$$|T_{n,k}| = \frac{L_n^{-1}}{M_{n,k}} |L_n S_{n,k}| I_{\mathcal{B}_n^c} + |T_{n,k}| I_{\mathcal{B}_n} \leq C\delta_n + \max_{1 \leq k \leq K_n} |T_{n,k}| I_{\mathcal{B}_n}. \quad (21)$$

For the first term on the right of (21) to converge, M_n must converge at a rate faster than $(nK_n)^{1/2}$. For the second term, using (20), observe that

$$\begin{aligned} \mathbb{P}(\mathcal{B}_n) &= \mathbb{P}\left(\bigcup_{k=1}^{K_n} \mathcal{B}_{n,k}\right) \\ &= \mathbb{P}\left\{\max_{1 \leq k \leq K_n} |L_n S_{n,k}| \geq C\right\} \\ &\leq \sum_{k=1}^{K_n} \mathbb{P}\{|L_n S_{n,k}| \geq C\} \leq \frac{K_n \sigma^2}{C^2 K_n} = \frac{\sigma^2}{C^2}. \end{aligned}$$

Therefore using Markov's inequality, we have for each $\varepsilon > 0$,

$$\begin{aligned} \mathbb{P}\left\{\max_{1 \leq k \leq K_n} |T_{n,k}| I_{\mathcal{B}_n} \geq \varepsilon\right\} &\leq \frac{\sum_{k=1}^{K_n} \mathbb{E}(|T_{n,k}| I_{\mathcal{B}_n})}{\varepsilon} \\ &\leq \frac{\sum_{k=1}^{K_n} \sqrt{\mathbb{E}(T_{n,k}^2) \mathbb{P}(\mathcal{B}_n)}}{\varepsilon} \quad (\text{Cauchy-Schwarz}) \\ &\leq \frac{\sigma}{C\varepsilon} \sum_{k=1}^{K_n} \sqrt{\mathbb{E}(T_{n,k}^2)} \quad (\text{bound from } \mathbb{P}(\mathcal{B}_n) \text{ above}). \end{aligned}$$

Because $\mathbb{E}(T_{n,k}^2) \leq M_n^{-2} \sum_{i=1}^n \mathbb{E}[(Z_{i,k}^{(n)})^2] \leq M_n^{-2} n\sigma^2$,

$$\mathbb{P}\left\{\max_{1 \leq k \leq K_n} |T_{n,k}| I_{\mathcal{B}_n} \geq \varepsilon\right\} \leq \frac{\sigma^2 n^{1/2} K_n}{C\varepsilon M_n}.$$

Therefore if $M_n^{-1} n^{1/2} K_n \rightarrow 0$, then by (21) we have shown

$$|T_{n,k}| \leq C\delta_n + o_p(C^{-1}\sigma^2 M_n^{-1} n^{1/2} K_n)$$

uniformly over k . But notice that $M_n^{-1} n^{1/2} K_n = K_n^{1/2} \delta_n \geq C\delta_n$ eventually, thus we have proven the following lemma.

LEMMA B.1. *If $M_n \uparrow \infty$ such that $M_n^{-1} n^{1/2} K_n \rightarrow 0$ then $|T_{n,k}| \leq o_p(1)$ uniformly over $k = 1, \dots, K_n$.*

APPENDIX C: CONSISTENCY FOR NOISE VARIABLES (PROOF OF THEOREM 3.1)

The idea for the proof is as follows. The two sums in the first square bracket of (19) will be dealt with by using Lemma B.1 (set $M_{n,k} = m_{n,k}$, $M_n = m_n$ and $Z_{i,k}^{(n)} = Z_i(\zeta_{n,k})$, then $T_{n,k}$ in Lemma B.1 equals $m_{n,k}^{-1} \sum_{i=1}^n Z_i(\zeta_{n,k})$). The term inside the second square bracket of (19) is a bias term and will be shown to be asymptotically equal to

$$\beta_{n,k}(S) = \mathbb{E}(\psi(\mathbf{X}^{(S)}) | \mathbf{X} \in R_{n,k}^S) - \mathbb{E}(\psi(\mathbf{X}^{(S)}) | \mathbf{X} \in R_{n,k}). \quad (22)$$

This will be shown to converge to zero for noise variables by using the smoothness assumptions for ψ and other conditions assumed by the theorem.

PROOF. Apply [Lemma B.1](#) to each of the sums in the first square bracket of (19). The lemma applies since $\{Z_i(\zeta_{n,k}), Z_i(\zeta_{n,k}^S)\}$ are centered i.i.d. variables with bounded second moment. The latter holds by Assumption (A1). For $\{Z_i(\zeta_{n,k})\}$, let $M_{n,k} = m_{n,k}, M_n = m_n$ where notice that $m_n^{-1}n^{1/2}K_n \rightarrow 0$ when $K_n \leq O(\log n)$ and $m_n = n^{1/2}\gamma_n$ where $\gamma_n \gg \log n$; thus verifying the rate condition of the lemma. Moreover, because $m_{k,n}^S \geq m_{k,n}$ since $R_{n,k} \subseteq R_{n,k}^S$, the conditions of the lemma also hold for $\{Z_i(\zeta_{n,k}^S)\}$ with $M_{n,k} = m_{n,k}^S, M_n = m_n$.

Therefore by [Lemma B.1](#), which holds uniformly,

$$\begin{aligned} \Delta_n(S) &\leq \sum_{k=1}^{K_n} W_{n,k} |o_p(1) + b_{n,k}| \\ &\leq o_p(1) + \sum_{k=1}^{K_n} W_{n,k} |b_{n,k}|, \quad \text{uniformly,} \end{aligned} \quad (23)$$

where (see the second term of (19) and use $\psi(\mathbf{X}) = \psi(\mathbf{X}^{(S)})$)

$$b_{n,k} = \frac{n}{m_{n,k}^S} \mathbb{E}[\psi(\mathbf{X}^{(S)}) I\{\mathbf{X} \in R_{n,k}^S\}] - \frac{n}{m_{n,k}} \mathbb{E}[\psi(\mathbf{X}^{(S)}) I\{\mathbf{X} \in R_{n,k}\}]. \quad (24)$$

Using [Lemma A.1](#) we will show (24) approximates

$$\begin{aligned} &\frac{\mathbb{E}[\psi(\mathbf{X}^{(S)}) I\{\mathbf{X} \in R_{n,k}^S\}]}{\mathbb{P}(R_{n,k}^S)} - \frac{\mathbb{E}[\psi(\mathbf{X}^{(S)}) I\{\mathbf{X} \in R_{n,k}\}]}{\mathbb{P}(R_{n,k})} \\ &= \mathbb{E}(\psi(\mathbf{X}^{(S)}) | \mathbf{X} \in R_{n,k}^S) - \mathbb{E}(\psi(\mathbf{X}^{(S)}) | \mathbf{X} \in R_{n,k}) \\ &:= \mathbb{E}_{n,k}^S(\psi) - \mathbb{E}_{n,k}(\psi), \end{aligned} \quad (25)$$

where for notational simplicity we write $\mathbb{E}_{n,k}^S$ and $\mathbb{E}_{n,k}$ for the conditional expectation of \mathbf{X} given $R_{n,k}^S$ and $R_{n,k}$. Observe that (25) is the asymptotic bias $\beta_{n,k} := \beta_{n,k}(S)$ discussed earlier in (22).

Apply [Lemma A.1](#) noting $m_{n,k} \geq m_n = n^{1/2}\gamma_n \gg \sqrt{n \log \log n}$. By (17), there exists a set \mathcal{A}_n with probability tending to one, such that

$$\frac{n}{m_{n,k}} = \frac{1}{\mathbb{P}(R_{n,k})} + \frac{\xi_{n,k}^*}{\mathbb{P}(R_{n,k})}, \quad \text{where } |\xi_{n,k}^*| \leq \xi_n^* = \gamma_n^{-1} \sqrt{\log \log n} \rightarrow 0.$$

In a similar fashion, using $m_{n,k}^S \geq m_{n,k} \geq m_n = n^{1/2}\gamma_n$, there exists a set \mathcal{A}_n^S with probability tending to one, such that

$$\frac{n}{m_{n,k}^S} = \frac{1}{\mathbb{P}(R_{n,k}^S)} + \frac{\xi_{n,k}^{*S}}{\mathbb{P}(R_{n,k}^S)}, \quad \text{where } |\xi_{n,k}^{*S}| \leq \xi_n^*.$$

Thus from (24), over the set $\mathcal{A}_n \cap \mathcal{A}_n^S$ (an event with probability tending to 1), we have

$$|b_{n,k}| = \left| \beta_{n,k} + \xi_{n,k}^{*S} \mathbb{E}_{n,k}^S(\psi) - \xi_{n,k}^* \mathbb{E}_{n,k}(\psi) \right| \leq |\beta_{n,k}| + \xi_n^* \left(|\mathbb{E}_{n,k}^S(\psi)| + |\mathbb{E}_{n,k}(\psi)| \right). \quad (26)$$

The smoothness assumption (A2) for ψ and the shrinking condition (A3) for $R_{n,k}$ are now used to expand $\mathbb{E}_{n,k}^S(\psi)$ and $\mathbb{E}_{n,k}(\psi)$ to first order which will show (25) is asymptotically

zero and will enable us to further bound (26). Let $\mathbf{x}_{n,k}$ be an arbitrary point in $R_{n,k}$. By the mean-value theorem, for each $\mathbf{x} \in R_{n,k}$ there exists a $\lambda_{n,k} \in [0, 1]$, such that

$$\psi(\mathbf{x}) - \psi(\mathbf{x}_{n,k}) = (\mathbf{x} - \mathbf{x}_{n,k})' \mathbf{f}(\mathbf{x}_{n,k}^*)$$

where $\mathbf{x}_{n,k}^* = \mathbf{x}_{n,k} + \lambda_{n,k}(\mathbf{x} - \mathbf{x}_{n,k})$ (note that the dependence of $\lambda_{n,k}$ on \mathbf{x} is suppressed). Using $\mathbf{f}(\mathbf{x}_{n,k}^*) = \mathbf{f}(\mathbf{x}_{n,k}) + [\mathbf{f}(\mathbf{x}_{n,k}^*) - \mathbf{f}(\mathbf{x}_{n,k})]$, the Lipschitz condition (12), and keeping in mind \mathbf{f} is zero over the coordinates for \mathcal{N} ,

$$|\psi(\mathbf{x}) - \psi(\mathbf{x}_{n,k})| \leq |(\mathbf{x}^{(S)} - \mathbf{x}_{n,k}^{(S)})' \mathbf{f}^{(S)}(\mathbf{x}_{n,k})| + C_0 |(\mathbf{x}^{(S)} - \mathbf{x}_{n,k}^{(S)})'| |(\mathbf{x}_{n,k}^{*(S)} - \mathbf{x}_{n,k}^{(S)})|.$$

Applying the Cauchy-Schwarz inequality to the first term on the right, and using assumption (A3), we have for $\mathbf{x} \in R_{n,k}$

$$\begin{aligned} |\psi(\mathbf{x}) - \psi(\mathbf{x}_{n,k})| &\leq \|(\mathbf{x}^{(S)} - \mathbf{x}_{n,k}^{(S)})\|_2 \|\mathbf{f}^{(S)}(\mathbf{x}_{n,k})\|_2 + C_0 |(\mathbf{x}^{(S)} - \mathbf{x}_{n,k}^{(S)})'| |(\mathbf{x}_{n,k}^{*(S)} - \mathbf{x}_{n,k}^{(S)})| \\ &\leq \text{diam}_S(R_{n,k}) \left[\|\mathbf{f}^{(S)}(\mathbf{x}_{n,k})\|_2 + C_0 \right] \\ &\leq r_n \left[\|\mathbf{f}^{(S)}(\mathbf{x}_{n,k})\|_2 + C_0 \right] = r_n \left[\|\mathbf{f}(\mathbf{x}_{n,k})\|_2 + C_0 \right]. \end{aligned} \quad (27)$$

Therefore $\mathbb{E}_{n,k}(\psi) = \psi(\mathbf{x}_{n,k}) + r_{n,k}$, where

$$|r_{n,k} := \mathbb{E}_{n,k}(\psi(\mathbf{X}) - \psi(\mathbf{x}_{n,k}))| \leq r_n \left[\|\mathbf{f}(\mathbf{x}_{n,k})\|_2 + C_0 \right] := r_{n,k}^*.$$

By a similar argument, $\mathbb{E}_{n,k}^S(\psi) = \psi(\mathbf{x}_{n,k}) + r_{n,k}^S$ where $|r_{n,k}^S| \leq r_{n,k}^*$ satisfies the same bound as $r_{n,k}$. This is because (27) holds for $\mathbf{x} \in R_{n,k}^S$ because $R_{n,k}^S$ only differs from $R_{n,k}$ along the noise coordinates (since $S \subseteq \mathcal{N}$).

Therefore $\mathbb{E}_{n,k}^S(\psi) = \psi(\mathbf{x}_{n,k}) + r_{n,k}^S$ and $\mathbb{E}_{n,k}(\psi) = \psi(\mathbf{x}_{n,k}) + r_{n,k}$, and hence

$$\beta_{n,k} = [\psi(\mathbf{x}_{n,k}) + r_{n,k}^S] - [\psi(\mathbf{x}_{n,k}) + r_{n,k}] = r_{n,k}^S - r_{n,k},$$

and (26) can be further bounded as follows:

$$\begin{aligned} |b_{n,k}| &\leq |r_{n,k}^S| + |r_{n,k}| + \xi_n^* \left(|\psi(\mathbf{x}_{n,k}) + r_{n,k}^S| + |\psi(\mathbf{x}_{n,k}) + r_{n,k}| \right) \\ &\leq 2(1 + \xi_n^*) r_{n,k}^* + 2\xi_n^* |\psi(\mathbf{x}_{n,k})|. \end{aligned}$$

Hence by (23), and assumption (A4), with probability tending to 1,

$$\begin{aligned} \Delta_n(S) &\leq o_p(1) + 2(1 + \xi_n^*) r_n \sum_{k=1}^{K_n} W_{n,k} \left[\|\mathbf{f}(\mathbf{x}_{n,k})\|_2 + C_0 \right] \\ &\quad + 2\xi_n^* \sum_{k=1}^{K_n} W_{n,k} |\psi(\mathbf{x}_{n,k})| \\ &\leq o_p(1) + O(r_n) + O(\xi_n^*) = o_p(1), \end{aligned}$$

where the convergence is uniform. \square

APPENDIX D: LIMITING BEHAVIOR FOR SIGNAL FEATURES (PROOF OF THEOREM 3.2)

The proof for $S = \{s\}$ a signal variable is similar to the noise variable case. The key difference is dealing with the bias term $\beta_{n,k} := \beta_{n,k}(s)$ (22) which is no longer asymptotically zero.

PROOF. Adopting the same notation as in the proof of [Theorem 3.1](#), let $\mathbb{E}_{n,k}$ and $\mathbb{E}_{n,k}^s$ be the conditional expectation for \mathbf{X} in $R_{n,k}$ and $R_{n,k}^s$. The same bound (27) used to derive $\mathbb{E}_{n,k}(\psi)$ applies here. Thus $\psi(\mathbf{x}) = \psi(\mathbf{x}_{n,k}) + r_{n,k}(\mathbf{x})$ where $|r_{n,k}(\mathbf{x})| \leq r_{n,k}^*$ for $\mathbf{x} \in R_{n,k}$ and $\mathbb{E}_{n,k}(\psi) = \psi(\mathbf{x}_{n,k}) + r_{n,k}$ where $r_{n,k} = \mathbb{E}_{n,k}(r_{n,k}(\mathbf{X})) \leq r_{n,k}^*$.

The previous argument used for $\mathbb{E}_{n,k}^s(\psi)$ however no longer applies because the released region now contains a signal variable. To deal with this, let $R_{n,k} = A_{n,k} \times B_{n,k}$ where $A_{n,k} = \times_{l=1}^d I_{n,k,l}$ is the subspace of $R_{n,k}$ defined by the signal features. By assumption (A3), $R_{n,k}$ is shrinking to zero in the signal features, thus $I_{n,k,l}$ are shrinking intervals for $l = 1, \dots, d$. On the other hand, $R_{n,k}^s$ releases the coordinates in the direction of s and therefore it is shrinking in the signal coordinates in all directions except the s direction. This is the subspace $A_{n,k}^s = \times_{l \in \mathcal{S} \setminus s} I_{n,k,l}$. Notice that $A_{n,k}^s$ can be written as the union of two disjoint regions

$$A_{n,k}^s = A_{n,k} \bigcup A_{n,k}^{*s}, \quad \text{where } A_{n,k}^{*s} = \times_{l=1}^{s-1} I_{n,k,l} \times I_{n,k,s}^c \times_{l=s+1}^d I_{n,k,l}$$

and in particular this implies

$$I\{\mathbf{x}^{(s)} \in A_{n,k}^s\} = I\{\mathbf{x}^{(s)} \in A_{n,k}\} + I\{\mathbf{x}^{(s)} \in A_{n,k}^{*s}\}. \quad (28)$$

For $\mathbf{x} \in R_{n,k}^s$,

$$\psi(\mathbf{x}) = [\psi(\mathbf{x}_{n,k}) + r_{n,k}(\mathbf{x})] I\{\mathbf{x}^{(s)} \in A_{n,k}\} + \psi(\mathbf{x}) I\{\mathbf{x}^{(s)} \in A_{n,k}^{*s}\}.$$

Using (28), with some rearrangement, this implies for each $\mathbf{x} \in R_{n,k}^s$

$$\begin{aligned} \psi(\mathbf{x}) &= \psi(\mathbf{x}_{n,k}) I\{\mathbf{x}^{(s)} \in A_{n,k}^s\} \\ &\quad + r_{n,k}(\mathbf{x}) I\{\mathbf{x}^{(s)} \in A_{n,k}\} \\ &\quad - [\psi(\mathbf{x}) - \psi(\mathbf{x}_{n,k})] I\{\mathbf{x}^{(s)} \in A_{n,k}\} \\ &\quad + [\psi(\mathbf{x}) - \psi(\mathbf{x}_{n,k})] I\{\mathbf{x}^{(s)} \in A_{n,k}^s\}. \end{aligned}$$

Therefore integrating with respect to $\mathbb{E}_{n,k}^s$,

$$\begin{aligned} \mathbb{E}_{n,k}^s(\psi(\mathbf{X})) &= \psi(\mathbf{x}_{n,k}) \\ &\quad + r_{n,k}^s \\ &\quad - \mathbb{E}_{n,k}^s \left([\psi(\mathbf{X}) - \psi(\mathbf{x}_{n,k})] I\{\mathbf{X}^{(s)} \in A_{n,k}\} \right) \\ &\quad + \mathbb{E}_{n,k}^s \left(\psi(\mathbf{X}) - \psi(\mathbf{x}_{n,k}) \right) \end{aligned} \quad (29)$$

where $r_{n,k}^s = \mathbb{E}_{n,k}^s(r_{n,k}(\mathbf{X}) I\{\mathbf{X}^{(s)} \in A_{n,k}\})$ and notice that

$$|r_{n,k}^s| \leq \mathbb{E}_{n,k}^s(r_{n,k}^* I\{\mathbf{X}^{(s)} \in A_{n,k}\}) \leq r_{n,k}^* \mathbb{E}_{n,k}^s(I\{\mathbf{X}^{(s)} \in A_{n,k}^s\}) = r_{n,k}^*.$$

In the proof of [Theorem 3.1](#) it was shown $|\psi(\mathbf{x}) - \psi(\mathbf{x}_{n,k})| \leq r_{n,k}^*$ for $\mathbf{x} \in R_{n,k}$. Therefore the third term of (29) is a remainder term of order $r_{n,k}^*$.

This leaves the fourth term in (29). To handle this, consider the local behavior of $\psi(\mathbf{x})$ for $\mathbf{x} \in A_{n,k}^s$ around the point $\tilde{\mathbf{x}}_{n,k} = (x_{n,k}^{(1)}, \dots, x_{n,k}^{(s-1)}, x_{n,k}^{(s)}, x_{n,k}^{(s+1)}, \dots, x_{n,k}^{(p)})' \in A_{n,k}^s$. By the mean-value theorem there exists a point $\tilde{\mathbf{x}}_{n,k}^* = \tilde{\mathbf{x}}_{n,k} + \lambda_{n,k}(\mathbf{x} - \tilde{\mathbf{x}}_{n,k})$ for some $0 \leq \lambda_{n,k} \leq 1$, such that

$$\psi(\mathbf{x}) - \psi(\tilde{\mathbf{x}}_{n,k}) = (\mathbf{x} - \tilde{\mathbf{x}}_{n,k})' \mathbf{f}(\tilde{\mathbf{x}}_{n,k}^*).$$

Because coordinate s of $\mathbf{x} - \tilde{\mathbf{x}}_{n,k}$ is zero,

$$\begin{aligned} |\psi(\mathbf{x}) - \psi(\tilde{\mathbf{x}}_{n,k})| &= \left| \sum_{l \in S \setminus s} \left((x^{(l)} - x_{n,k}^{(l)}) \mathbf{f}^{(l)}(\tilde{\mathbf{x}}_{n,k}^*) \right) \right| \\ &\leq \sum_{l \in S \setminus s} \left(|x^{(l)} - x_{n,k}^{(l)}| \cdot |\mathbf{f}^{(l)}(\tilde{\mathbf{x}}_{n,k}^*)| \right) \\ &\leq \sum_{l \in S \setminus s} \left(|x^{(l)} - x_{n,k}^{(l)}| \cdot |\mathbf{f}^{(l)}(\tilde{\mathbf{x}}_{n,k}^*)| \right) + |\tilde{x} - x_{n,k}^{(s)}| \cdot |\mathbf{f}^{(s)}(\tilde{\mathbf{x}}_{n,k}^*)| \\ &= |(\tilde{\mathbf{x}} - \mathbf{x}_{n,k}^{(s)})'| |\mathbf{f}^{(s)}(\tilde{\mathbf{x}}_{n,k}^*)| \end{aligned}$$

where $\tilde{\mathbf{x}} = (x^{(1)}, \dots, x^{(s-1)}, \tilde{x}, x^{(s+1)}, \dots, x^{(p)})'$ and \tilde{x} can be chosen to be an arbitrary value in $I_{n,k,s}$. Notice that $\tilde{\mathbf{x}} \in A_{n,k}$. Therefore the right-hand side can be bounded using the argument of [Theorem 3.1](#) from which it follows that

$$\left| \psi(\mathbf{x}) - \psi(\tilde{\mathbf{x}}_{n,k}) \right| \leq r_{n,k}^*, \quad \text{for } \mathbf{x} \in A_{n,k}^s.$$

Recall that $\psi_{n,k}^s(z) = \psi(x_{n,k}^{(1)}, \dots, x_{n,k}^{(s-1)}, z, x_{n,k}^{(s+1)}, \dots, x_{n,k}^{(d)})$. Therefore, $\psi(\tilde{\mathbf{x}}_{n,k}) = \psi_{n,k}^s(x^{(s)})$ and $\psi(\mathbf{x}_{n,k}) = \psi_{n,k}^s(x_{n,k}^{(s)})$, from which it follows

$$\mathbb{E}_{n,k}^s \left(\psi(\mathbf{X}) - \psi(\mathbf{x}_{n,k}) \right) = \mathbb{E}_{n,k}^s \left(\psi_{n,k}^s(X^{(s)}) - \psi_{n,k}^s(x_{n,k}^{(s)}) \right) + O(r_{n,k}^*), \quad (30)$$

and hence using [\(29\)](#),

$$\begin{aligned} \beta_{n,k} &= \mathbb{E}_{n,k}^S(\psi) - \mathbb{E}_{n,k}(\psi) \\ &= \left[\psi(\mathbf{x}_{k,n}) + \mathbb{E}_{n,k}^s \left(\psi_{n,k}^s(X^{(s)}) - \psi_{n,k}^s(x_{n,k}^{(s)}) \right) + O(r_{n,k}^*) \right] - \left[\psi(\mathbf{x}_{k,n}) + r_{n,k} \right] \\ &= \mathbb{E}_{n,k}^s \left(\psi_{n,k}^s(X^{(s)}) - \psi_{n,k}^s(x_{n,k}^{(s)}) \right) + O(r_{n,k}^*). \end{aligned}$$

Thus the bias does not vanish asymptotically as in the noise variable case.

To finish the proof we follow the rest of the proof of [Theorem 3.1](#). To simplify notation let $h_{n,k}(z) = \psi_{n,k}^s(z) - \psi_{n,k}^s(x_{n,k}^{(s)})$. Then

$$\begin{aligned} \Delta_n(s) &= o_p(1) + \sum_{k=1}^{K_n} W_{n,k} \left| \beta_{n,k} + \xi_{n,k}^{*s} \mathbb{E}_{n,k}^s(\psi) - \xi_{n,k}^* \mathbb{E}_{n,k}(\psi) \right| \\ &= o_p(1) + \sum_{k=1}^{K_n} W_{n,k} \left| \beta_{n,k} + \xi_{n,k}^{*s} \mathbb{E}_{n,k}^s(\psi) \right| \\ &= o_p(1) + \sum_{k=1}^{K_n} W_{n,k} \left| (1 + \xi_{n,k}^{*s}) \mathbb{E}_{n,k}^s(h_{n,k}(X^{(s)})) \right| \\ &= o_p(1) + (1 + o_p(1)) \sum_{k=1}^{K_n} W_{n,k} \left| \mathbb{E}_{n,k}^s(h_{n,k}(X^{(s)})) \right|. \end{aligned}$$

Going from line two to line three, we have used $\xi_{n,k}^{*s} \mathbb{E}_{n,k}^s(\psi) = \xi_{n,k}^{*s} \mathbb{E}_{n,k}^s(h_{n,k}(X^{(s)})) + o_p(1)$, where the $o_p(1)$ term is uniform and is due to [\(29\)](#) combined with [\(30\)](#). Finally, the last line

holds because

$$\begin{aligned}
& (1 + \xi_n^*) \sum_{k=1}^{K_n} W_{n,k} \left| \mathbb{E}_{n,k}^s(h_{n,k}(X^{(s)})) \right| \\
& \geq \sum_{k=1}^{K_n} W_{n,k} \left| (1 + \xi_{n,k}^{*s}) \mathbb{E}_{n,k}^s(h_{n,k}(X^{(s)})) \right| \\
& \geq \sum_{k=1}^{K_n} W_{n,k} \left| \mathbb{E}_{n,k}^s(h_{n,k}(X^{(s)})) \right| - \xi_n^* \sum_{k=1}^{K_n} W_{n,k} \left| \mathbb{E}_{n,k}^s(h_{n,k}(X^{(s)})) \right| \\
& = (1 - \xi_n^*) \sum_{k=1}^{K_n} W_{n,k} \left| \mathbb{E}_{n,k}^s(h_{n,k}(X^{(s)})) \right|.
\end{aligned}$$

The right inequality is because $|a + b| \geq |a| - |b|$ for any real-valued a, b . \square

APPENDIX E: REGRESSION SYNTHETIC EXPERIMENTS USED FOR BENCHMARKING

Regression simulation models used to test VarPro are listed below:

1. *cobra2*: $\psi(\mathbf{x}) = x^{(1)}x^{(2)} + (x^{(3)})^2 - x^{(4)}x^{(7)} + x^{(8)}x^{(10)} - (x^{(6)})^2$, $X^{(j)} \sim U(-1, 1)$, $\varepsilon \sim N(0, 0.1^2)$.
2. *cobra8*: $\psi(\mathbf{x}, \varepsilon) = I\{x^{(1)} + (x^{(4)})^3 + x^{(9)} + \sin(x^{(2)}x^{(8)}) + \varepsilon > 0.38\}$, $X^{(j)} \sim U(-.25, 1)$, $\varepsilon \sim N(0, 0.1^2)$.
3. *friedman1*: $\psi(\mathbf{x}) = 10 \sin(\pi x^{(1)}x^{(2)}) + 20(x^{(3)} - 0.5)^2 + 10x^{(4)} + 5x^{(5)}$, $X^{(j)} \sim U(0, 1)$, $\varepsilon \sim N(0, 1)$.
4. *friedman3*: $\psi(\mathbf{x}) = \arctan \left[\frac{x^{(2)}x^{(3)} - 1/(x^{(2)}x^{(4)})}{x^{(1)}} \right]$, $X^{(1)} \sim U(0, 100)$, $X^{(2)} \sim U(40\pi, 560\pi)$, $X^{(3)}, \dots, X^{(p)} \sim U(0, 1)$, $\varepsilon \sim N(0, 1)$.
5. *inx1*: $\psi(\mathbf{x}) = x^{(1)}(x^{(2)})^2 \sqrt{|x^{(3)}|} + \lfloor x^{(4)} - x^{(5)}x^{(6)} \rfloor$, $X^{(j)} \sim U(-1, 1)$, $\varepsilon \sim N(0, 0.1^2)$.
6. *inx2*: $\psi(\mathbf{x}) = x^{(3)}(x^{(1)} + 1)^{|x^{(2)}|} - \sqrt{\frac{(x^{(5)})^2}{|x^{(4)}| + |x^{(5)}| + |x^{(6)}|}}$, $X^{(j)} \sim U(-1, 1)$, $\varepsilon \sim N(0, 0.1^2)$.
7. *inx3*: $\psi(\mathbf{x}) = \cos(x^{(1)} - x^{(2)}) + \arcsin(x^{(1)}x^{(3)}) - \arctan(x^{(2)} - (x^{(3)})^2)$, $X^{(j)} \sim U(-1, 1)$, $\varepsilon \sim N(0, 0.1^2)$.
8. *lm*: $\psi(\mathbf{x}) = \sum_{j=1}^{15} x^{(j)}$, $X^{(j)} \sim N(0, 1)$, $\varepsilon \sim N(0, 15^2)$.
9. *lmi1*: $\psi(\mathbf{x}) = .05f_1(\mathbf{x}) + \exp(.02f_1(\mathbf{x})f_2(\mathbf{x}))$, where $f_1(\mathbf{x}) = \sum_{j=1}^{10} x^{(j)}$, $f_2(\mathbf{x}) = \sum_{j=11}^{20} x^{(j)}$, $X^{(j)} \sim U(0, 1)$, $\varepsilon \sim N(0, .1^2)$.
10. *lmi2*: $\psi(\mathbf{x}) = 3(\sum_{j=1}^{15} x^{(j)})^2$, $X^{(j)} \sim N(0, 1)$, $\varepsilon \sim N(0, 15^2)$.
11. *sup*: $\psi(\mathbf{x}) = 10x^{(1)}x^{(2)} + .25 \frac{1}{x^{(3)}x^{(4)} + 10x^{(5)}x^{(6)}}$, $X^{(j)} \sim U(0.05, 1)$, $\varepsilon \sim N(0, 0.5^2)$.
12. *sup2*: $\psi(\mathbf{x}) = \pi^{x^{(1)}x^{(2)}} \sqrt{2x^{(3)}} - \arcsin(x^{(4)}) + \log(x^{(3)} + x^{(5)}) - \frac{x^{(9)}}{x^{(10)}} \sqrt{\frac{x^{(7)}}{x^{(8)}}} - x^{(2)}x^{(7)}$, $X^{(j)} \sim U(0.5, 1)$, $\varepsilon \sim N(0, 0.5^2)$.
13. *supX*: Same as *sup* but with smaller N and larger p .
14. *supX2*: Same as *sup2* but with smaller N and larger p .

Simulations *cobra* are from [3] and *friedman* are from [19]. All experiments used $N = 2000$ and $p = 40$ except for *supX* and *sup2X* where $N = 500$ and $p = 200$. In a first set of runs, features were independently sampled as described above. In a second run, all features retained the same marginal distribution as before, but were transformed using a copula so as to make all features correlated with correlation $\rho = 0.9$. This was done for all simulations except *lm* and *lmi2* where the 15 signal features $X^{(1)}, \dots, X^{(15)}$ were correlated within blocks of size 5 (1–5, 6–10 and 11–15).

E.1. Additional simulations. Synthetic data was also obtained using the function `regDataGen` from the R-package `CORElearn`. In these experiments, the response is randomly selected from two different functions. The choice depends on a “switch variable” which determines whether $\psi(\mathbf{x}) = x^{(4)} - 2x^{(5)} + 3x^{(6)}$ or $\psi(\mathbf{x}) = \cos(4\pi x^{(4)})(2x^{(5)} - 3x^{(6)})$. Therefore, half the time the model is linear and half the time it is nonlinear. Also there are 4 discrete variables a_1, a_2, a_3, a_4 , the first two a_1, a_2 carry information about the switch variable. Variables $X^{(1)}, X^{(2)}$ also carry information about the hidden variable. The simulation was modified to allow for additional noise variables drawn from a $U(0, 1)$ distribution. Different N and p and varying configurations for information about the hidden variable were used. The following simulations were considered:

15. *corelearn1*: a_1, a_2 and $X^{(1)}, X^{(2)}$ contain no information; $N = 300$.
16. *corelearn2*: a_1, a_2 and $X^{(1)}, X^{(2)}$ contain no information; $N = 200$.
17. *corelearn3*: a_1, a_2 contain full information and $X^{(1)}, X^{(2)}$ contain no information; $N = 100$.
18. *corelearn4*: a_1, a_2 and $X^{(1)}, X^{(2)}$ contain full information; $N = 100$.
19. *corelearn5*: a_1, a_2 and $X^{(1)}, X^{(2)}$ contain full information; $N = 100$; 50 noise variables added.
20. *corelearn6*: a_1, a_2 and $X^{(1)}, X^{(2)}$ contain full information; $N = 100$; 200 noise variables added.

In the first set of runs, features were sampled as described in `regDataGen`. In the second run, all features retained the same marginal distribution as before, but were transformed to have correlation $\rho = 0.9$. Note that signal variables for the first two simulations are $X^{(4)}, X^{(5)}, X^{(6)}$ while the third simulation adds a_1, a_2 and the last three simulations adds a_1, a_2 and $X^{(1)}, X^{(2)}$ as signals.

APPENDIX F: ASYMPTOTICS FOR THE MODIFIED PROCEDURE (PROOF OF THEOREM 5.1)

The following assumption will be used in the proof:

- (A5) There exists a sequence $\tilde{r}_n \rightarrow 0$ and subspace $\mathcal{X}_n \subseteq \mathcal{X}$ containing all regions $\bigcup_{k=1}^{K_n} R_{k,n}$ and released regions $\bigcup_{k=1}^{K_n} R_{n,k}^S$ such that $|\psi_n(\mathbf{x}) - \psi(\mathbf{x})| \leq \tilde{r}_n$ for $\mathbf{x} \in \mathcal{X}_n$.

The assumption requires ψ_n to converge uniformly to ψ but some flexibility is allowed in that convergence only has to hold over a suitably defined subspace. For example, if $\psi_n(\mathbf{x}) = h(\sum_{l=1}^p \alpha_{n,l} x^{(l)})$ and $\psi(\mathbf{x}) = h(\sum_{l=1}^p \alpha_{0,l} x^{(l)})$ for h a real-valued function with derivative h' , then by the mean value theorem

$$\begin{aligned} |\psi_n(\mathbf{x}) - \psi(\mathbf{x})| &\leq \left| h' \left(\sum_{l=1}^p \alpha_{n,l}^* x^{(l)} \right) \right| \sum_{l=1}^p |x^{(l)} (\alpha_{n,l} - \alpha_{0,l})| \\ &\leq \left| h' \left(\sum_{l=1}^p \alpha_{n,l}^* x^{(l)} \right) \right| \cdot \|\mathbf{x}\|_2 \cdot \sqrt{\sum_{l=1}^p |\alpha_{n,l} - \alpha_{0,l}|^2} \end{aligned}$$

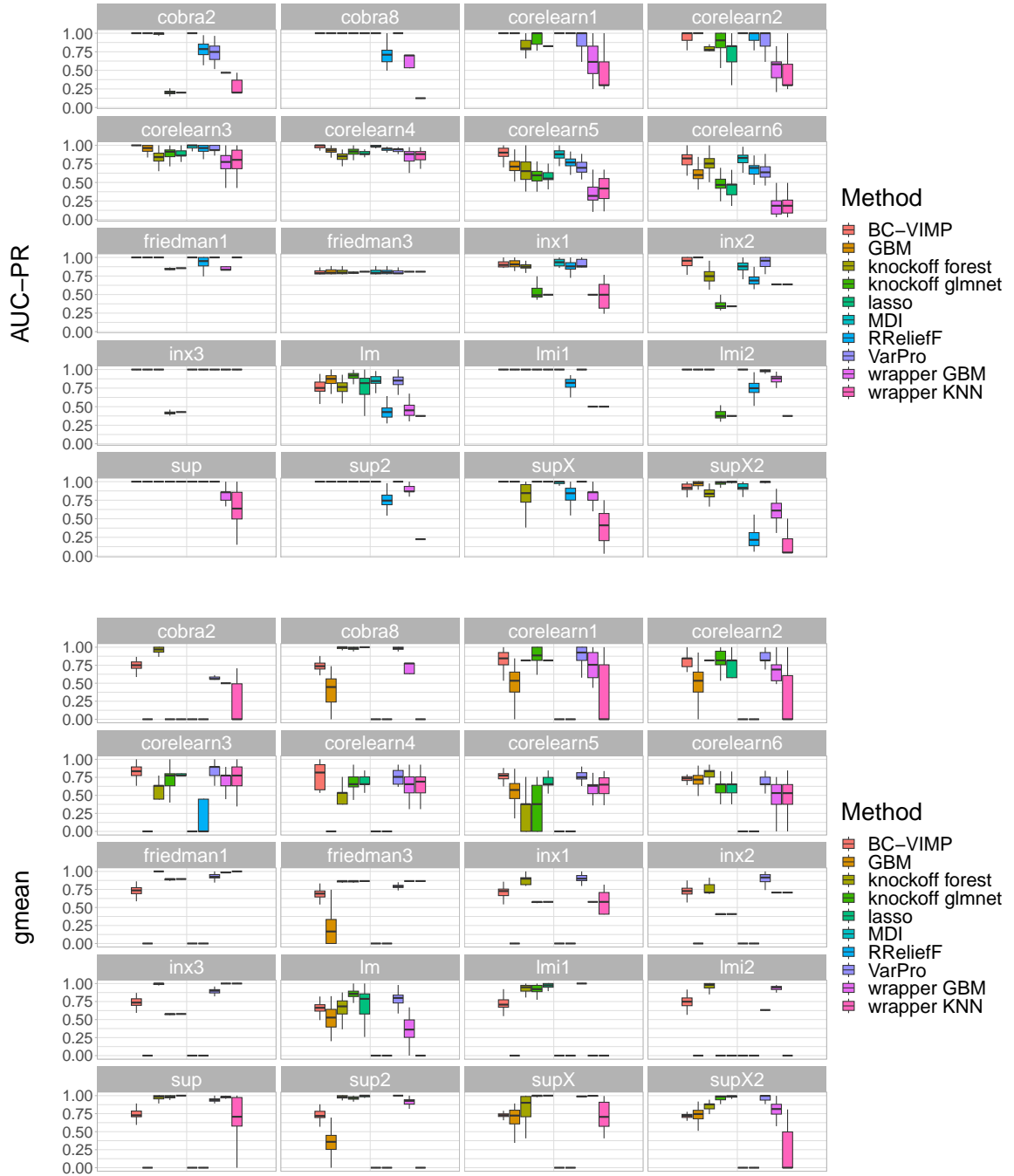


FIG E1. Area under the precision recall curve (AUC-PR) and gmean (geometric mean of TPR and TNR) feature selection performance in regression simulations where variables are uncorrelated.

where $\alpha_{n,l}^*$ is some value between $\alpha_{n,l}$ and $\alpha_{0,l}$. The simplest way to satisfy (A5) is to require boundedness where $\mathcal{X}_n \subseteq \mathcal{X}_0$ for \mathcal{X}_0 a closed bounded subspace of \mathcal{X} . Then (A5) holds under the relatively mild assumptions that h' is continuous and $\sum_{l=1}^p |\alpha_{n,l} - \alpha_{0,l}| \rightarrow 0$ where convergence can be at any rate. The boundedness condition is easily met as the size of a region is entirely controlled by the data analyst.

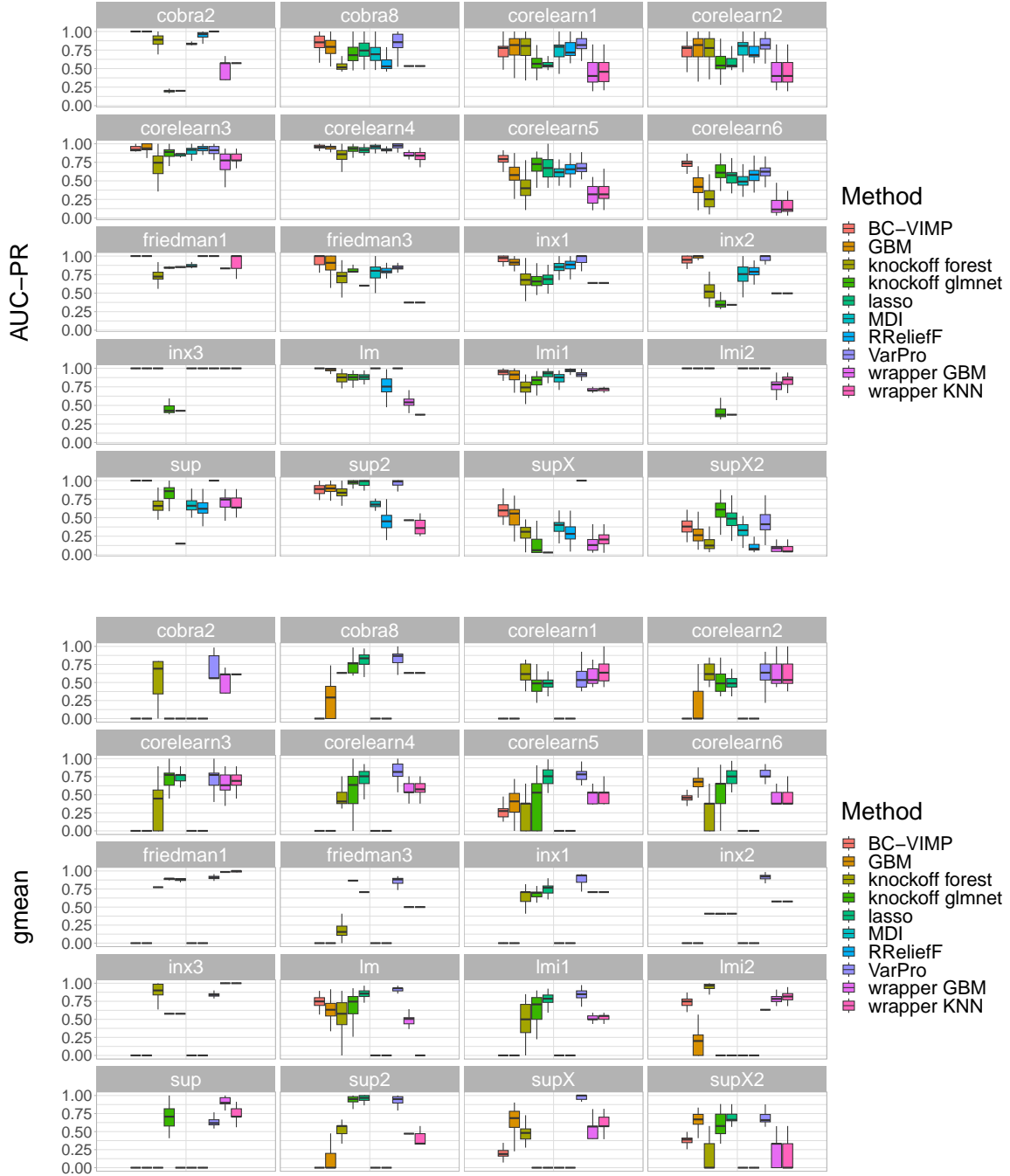


FIG E2. Similar to Fig. E1 but using correlated variables.

PROOF. For the proof we use a centering argument for $\tilde{\Delta}_n(S)$ similar to that used for $\Delta_n(S)$. Let $Z_i^*(\zeta) = \psi(\mathbf{X}_i)I\{\mathbf{X}_i \in R(\zeta)\} - b(\zeta)$ where $b(\zeta) = \mathbb{E}[\psi(\mathbf{X})I\{\mathbf{X} \in R(\zeta)\}]$. Using $\psi_n = \psi + (\psi_n - \psi)$, it follows that

$$|\tilde{\theta}_n(\zeta_{n,k}^S) - \tilde{\theta}_n(\zeta_{n,k})| = \left| \frac{1}{m_{n,k}^S} \sum_{i=1}^n Z_i^*(\zeta_{n,k}^S) - \frac{1}{m_{n,k}} \sum_{i=1}^n Z_i^*(\zeta_{n,k}) \right|$$

$$\begin{aligned}
& + \left[\frac{nb(\zeta_{n,k}^S)}{m_{n,k}^S} - \frac{nb(\zeta_{n,k})}{m_{n,k}} \right] \\
& + \left[\frac{1}{m_{n,k}^S} \sum_{i=1}^n \tilde{Z}_{n,i}(\zeta_{n,k}^S) - \frac{1}{m_{n,k}} \sum_{i=1}^n \tilde{Z}_{n,i}(\zeta_{n,k}) \right], \quad (31)
\end{aligned}$$

where $\tilde{Z}_{n,i}(\zeta) = [\psi_n(\mathbf{X}_i) - \psi(\mathbf{X}_i)]I\{\mathbf{X}_i \in R(\zeta)\}$. Observe that the second term in (31) is the bias term asymptotically equal to $\beta_{n,k}(S)$ (22) worked out in the previous theorems. The terms in the first square bracket in (31) are sums of i.i.d. centered variables and therefore are similar to the sums in (19) and can be dealt with by Lemma B.1 to show they converge to zero uniformly in probability. Therefore we only need consider the terms inside the third bracket of (31).

Therefore, consider the bound

$$\begin{aligned}
& \sum_{k=1}^{K_n} W_{n,k} \left| \frac{1}{m_{n,k}^S} \sum_{i=1}^n \tilde{Z}_{n,i}(\zeta_{n,k}^S) - \frac{1}{m_{n,k}} \sum_{i=1}^n \tilde{Z}_{n,i}(\zeta_{n,k}) \right| \\
& \leq \sum_{k=1}^{K_n} \frac{W_{n,k}}{m_{n,k}^S} \sum_{i=1}^n |\tilde{Z}_{n,i}(\zeta_{n,k}^S)| + \sum_{k=1}^{K_n} \frac{W_{n,k}}{m_{n,k}} \sum_{i=1}^n |\tilde{Z}_{n,i}(\zeta_{n,k})|. \quad (32)
\end{aligned}$$

Begin with the first sum on the right of (32). By (A5),

$$|\tilde{Z}_{n,i}(\zeta_{n,k}^S)| \leq |\psi_n(\mathbf{X}_i) - \psi(\mathbf{X}_i)|I\{\mathbf{X}_i \in R_{n,k}^S\} \leq \tilde{r}_n I\{\mathbf{X}_i \in R_{n,k}^S\}.$$

Therefore

$$\sum_{k=1}^{K_n} \frac{W_{n,k}}{m_{n,k}^S} \sum_{i=1}^n |\tilde{Z}_{n,i}(\zeta_{n,k}^S)| \leq r_n \sum_{k=1}^{K_n} \frac{W_{n,k}}{m_{n,k}^S} \sum_{i=1}^n I\{\mathbf{X}_i \in R_{n,k}^S\} = r_n \rightarrow 0.$$

The second sum on the right of (32) involving $\tilde{Z}_{n,i}(\zeta_{n,k})$ is dealt with similarly. \square

Code Availability. Our code is publicly available as an R-package `varPro` and is available at the repository <https://github.com/kogalur/varPro>.

Funding. Research for the authors was supported by the National Institute Of General Medical Sciences of the National Institutes of Health, Award Number R35 GM139659 and the National Heart, Lung, and Blood Institute of the National Institutes of Health, Award Number R01 HL164405.

REFERENCES

- [1] ANDERSEN, P. K., HANSEN, M. G. and KLEIN, J. P. (2004). Regression analysis of restricted mean survival time based on pseudo-observations. *Lifetime Data Analysis* **10** 335–350.
- [2] BIAU, G., DEVROYE, L. and LUGOSI, G. (2008). Consistency of random forests and other averaging classifiers. *Journal of Machine Learning Research* **9** 2015–2033.
- [3] BIAU, G., FISCHER, A., GUEDJ, B. and MALLEY, J. D. (2016). COBRA: A combined regression strategy. *Journal of Multivariate Analysis* **146** 18–28.
- [4] BISCHL, B., LANG, M., KOTTHOFF, L., SCHIFFNER, J., RICHTER, J., STUDERUS, E., CASALICCHIO, G. and JONES, Z. M. (2016). mlr: Machine Learning in R. *Journal of Machine Learning Research* **17** 1-5.
- [5] BREIMAN, L. (2001). Random forests. *Machine Learning* **45** 5–32.
- [6] BREIMAN, L. (2002). Manual on setting up, using, and understanding random forests v3. 1. *Statistics Department University of California Berkeley, CA, USA* **1**.

- [7] BREIMAN, L., FRIEDMAN, J., STONE, C. J. and OLSHEN, R. A. (1984). *Classification and Regression Trees*. CRC press.
- [8] CANDES, E., FAN, Y., JANSON, L. and LV, J. (2018). Panning for gold: ‘model-X’ knockoffs for high dimensional controlled variable selection. *Journal of the Royal Statistical Society: Series B (Statistical Methodology)* **80** 551–577.
- [9] CECCARELLI, M., BARTHEL, F. P., MALTA, T. M., SABEDOT, T. S., SALAMA, S. R., MURRAY, B. A., MOROZOVA, O., NEWTON, Y., RADENBAUGH, A., PAGNOTTA, S. M. et al. (2016). Molecular profiling reveals biologically discrete subsets and pathways of progression in diffuse glioma. *Cell* **164** 550–563.
- [10] CHEN, R.-C., DEWI, C., HUANG, S.-W. and CARAKA, R. E. (2020). Selecting critical features for data classification based on machine learning methods. *Journal of Big Data* **7** 52.
- [11] CHIPMAN, H. A., GEORGE, E. I. and MCCULLOCH, R. E. (2010). BART: Bayesian additive regression trees. *The Annals of Applied Statistics* **4** 266–298.
- [12] COLE, C. R., FOODY, J. M., BLACKSTONE, E. H. and LAUER, M. S. (2000). Heart rate recovery after submaximal exercise testing as a predictor of mortality in a cardiovascularly healthy cohort. *Annals of Internal Medicine* **132** 552–555.
- [13] DEVROYE, L., GYÖRFI, L. and LUGOSI, G. (2013). *A Probabilistic Theory of Pattern Recognition* **31**. Springer.
- [14] DOKSUM, K., TANG, S. and TSUI, K.-W. (2008). Nonparametric variable selection: the EARTH algorithm. *Journal of the American Statistical Association* **103** 1609–1620.
- [15] DRAMIŃSKI, M. and KORONACKI, J. (2018). rmcfs: an R package for Monte Carlo feature selection and interdependency discovery. *Journal of Statistical Software* **85** 1–28.
- [16] FAN, J. and LV, J. (2008). Sure independence screening for ultrahigh dimensional feature space. *Journal of the Royal Statistical Society Series B: Statistical Methodology* **70** 849–911.
- [17] FISHER, A., RUDIN, C. and DOMINICI, F. (2019). All Models are Wrong, but Many are Useful: Learning a Variable’s Importance by Studying an Entire Class of Prediction Models Simultaneously. *Journal of Machine Learning Research* **20** 1–81.
- [18] FRIEDMAN, J., HASTIE, T. and TIBSHIRANI, R. (2010). Regularization paths for generalized linear models via coordinate descent. *Journal of Statistical Software* **33** 1–22.
- [19] FRIEDMAN, J. H. (1991). Multivariate adaptive regression splines. *The Annals of Statistics* **19** 1–67.
- [20] FRIEDMAN, J. H. (2001). Greedy function approximation: a gradient boosting machine. *Annals of Statistics* **29** 1189–1232.
- [21] FÜRNKRANZ, J. (1997). Pruning algorithms for rule learning. *Machine Learning* **27** 139–172.
- [22] GENUER, R., POGGI, J.-M. and TULEAU-MALOT, C. (2010). Variable selection using random forests. *Pattern Recognition Letters* **31** 2225–2236.
- [23] GERDS, T. A., CAI, T. and SCHUMACHER, M. (2008). The performance of risk prediction models. *Biometrical Journal: Journal of Mathematical Methods in Biosciences* **50** 457–479.
- [24] GERDS, T. A. and SCHUMACHER, M. (2006). Consistent estimation of the expected Brier score in general survival models with right-censored event times. *Biometrical Journal* **48** 1029–1040.
- [25] GRAF, E., SCHMOOR, C., SAUERBREI, W. and SCHUMACHER, M. (1999). Assessment and comparison of prognostic classification schemes for survival data. *Statistics in Medicine* **18** 2529–2545.
- [26] GREENWELL, B., BOEHMKE, B., CUNNINGHAM, J. and DEVELOPERS, G. (2020). gbm: Generalized Boosted Regression Models R package version 2.1.8.
- [27] GRÖMPING, U. (2009). Variable importance assessment in regression: linear regression versus random forest. *The American Statistician* **63** 308–319.
- [28] GUYON, I., WESTON, J., BARNHILL, S. and VAPNIK, V. (2002). Gene selection for cancer classification using support vector machines. *Machine learning* **46** 389–422.
- [29] GYÖRFI, L., KOHLER, M., KRZYŻAK, A., WALK, H. et al. (2002). *A Distribution-Free Theory of Non-parametric Regression* **1**. Springer.
- [30] HOEFFDING, W. (1963). Probability Inequalities for Sums of Bounded Random Variables. *Journal of the American Statistical Association* **58** 13–30.
- [31] HSICH, E., CHADALAVADA, S., KRISHNASWAMY, G., STARLING, R. C., POTHIER, C. E., BLACKSTONE, E. H. and LAUER, M. S. (2007). Long-term prognostic value of peak oxygen consumption in women versus men with heart failure and severely impaired left ventricular systolic function. *The American Journal of Cardiology* **100** 291–295.
- [32] IMAI, K., SATO, H., HORI, M., KUSUOKA, H., OZAKI, H., YOKOYAMA, H., TAKEDA, H., INOUE, M. and KAMADA, T. (1994). Vagally mediated heart rate recovery after exercise is accelerated in athletes but blunted in patients with chronic heart failure. *Journal of the American College of Cardiology* **24** 1529–1535.

- [33] IRWIN, J. O. (1949). The standard error of an estimate of expectation of life, with special reference to expectation of tumourless life in experiments with mice. *Epidemiology & Infection* **47** 188–189.
- [34] ISHWARAN, H. (2007). Variable importance in binary regression trees and forests. *Electronic Journal of Statistics* **1** 519–537.
- [35] ISHWARAN, H., BLACKSTONE, E. H., POTHIER, C. E. and LAUER, M. S. (2004). Relative risk forests for exercise heart rate recovery as a predictor of mortality. *Journal of the American Statistical Association* **99** 591–600.
- [36] ISHWARAN, H. and KOGALUR, U. B. (2023). Random Forests for Survival, Regression, and Classification (RF-SRC) R package version 3.2.2.
- [37] ISHWARAN, H., KOGALUR, U. B., BLACKSTONE, E. H. and LAUER, M. S. (2008). Random survival forests. *The Annals of Applied Statistics* **2** 841–860.
- [38] ISHWARAN, H., KOGALUR, U. B., CHEN, X. and MINN, A. J. (2011). Random survival forests for high-dimensional data. *Statistical Analysis and Data Mining: The ASA Data Science Journal* **4** 115–132.
- [39] ISHWARAN, H., KOGALUR, U. B., GORODESKI, E. Z., MINN, A. J. and LAUER, M. S. (2010). High-dimensional variable selection for survival data. *Journal of the American Statistical Association* **105** 205–217.
- [40] KIM, D. H., UNO, H. and WEI, L.-J. (2017). Restricted Mean Survival Time as a Measure to Interpret Clinical Trial Results. *JAMA Cardiology* **2** 1179–1180.
- [41] KIRA, K. and RENDELL, L. A. (1992). The feature selection problem: Traditional methods and a new algorithm. In *Proceedings of the Tenth National Conference on Artificial intelligence* 129–134.
- [42] KOHAVI, R. and JOHN, G. H. (1997). Wrappers for feature subset selection. *Artificial Intelligence* **97** 273–324.
- [43] KUBAT, M., HOLTE, R. and MATWIN, S. (1997). Learning when negative examples abound. In *European Conference on Machine Learning* 146–153. Springer.
- [44] KUHN, M. (2022). caret: Classification and Regression Training R package version 6.0-91.
- [45] KURSA, M. B. and RUDNICKI, W. R. (2010). Feature Selection with the Boruta Package. *Journal of Statistical Software* **36** 1–13.
- [46] LAGANI, V., ATHINEOU, G., FARCOMENI, A., TSAGRIS, M. and TSAMARDINOS, I. (2017). Feature Selection with the R Package MXM: Discovering Statistically Equivalent Feature Subsets. *Journal of Statistical Software* **80**. <https://doi.org/10.18637/jss.v080.i07>
- [47] LEE, K.-Y., LI, B. and ZHAO, H. (2016). Variable selection via additive conditional independence. *Journal of the Royal Statistical Society: Series B (Statistical Methodology)* **78** 1037–1055.
- [48] LEI, J., G’SELL, M., RINALDO, A., TIBSHIRANI, R. J. and WASSERMAN, L. (2018). Distribution-free predictive inference for regression. *Journal of the American Statistical Association* **113** 1094–1111.
- [49] LI, L., DENNIS COOK, R. and NACHTSHEIM, C. J. (2005). Model-free variable selection. *Journal of the Royal Statistical Society: Series B (Statistical Methodology)* **67** 285–299.
- [50] LIU, Y., ROČKOVÁ, V. and WANG, Y. (2021). Variable selection with ABC Bayesian forests. *Journal of the Royal Statistical Society: Series B (Statistical Methodology)* **83** 453–481.
- [51] LOUPPE, G., WEHENKEL, L., SUTERA, A. and GEURTS, P. (2013). Understanding variable importances in forests of randomized trees. *Advances in Neural Information Processing Systems* **26** 431–439.
- [52] NUTI, G., JIMÉNEZ RUGAMA, L. A. and CROSS, A.-I. (2021). An explainable Bayesian decision tree algorithm. *Frontiers in Applied Mathematics and Statistics* **7** 1–9.
- [53] PATTERSON, E. and SESIA, M. (2022). knockoff: The Knockoff Filter for Controlled Variable Selection R package version 0.3.5.
- [54] RAMÓN, D.-U. and ALVAREZ DE ANDRÉS, S. (2006). Gene selection and classification of microarray data using random forest. *BMC bioinformatics* **7** 1–13.
- [55] ROBNIK-ŠIKONJA, M., KONONENKO, I. et al. (1997). An adaptation of Relief for attribute estimation in regression. In *Machine learning: Proceedings of the fourteenth international conference (ICML’97)* **5** 296–304. Citeseer.
- [56] ROYSTON, P. and PARMAR, M. K. B. (2011). The use of restricted mean survival time to estimate the treatment effect in randomized clinical trials when the proportional hazards assumption is in doubt. *Statistics in Medicine* **30** 2409–2421.
- [57] SILVA, T. (2022). TCGAbiolinksGUI.data: Data for the TCGAbiolinksGUI package. R package version 1.14.1.
- [58] SIMON, N., FRIEDMAN, J., HASTIE, T. and TIBSHIRANI, R. (2011). Regularization paths for Cox’s proportional hazards model via coordinate descent. *Journal of Statistical Software* **39** 1–13.
- [59] STATNIKOV, A., LEMEIR, J. and ALIFERIS, C. F. (2013). Algorithms for discovery of multiple Markov boundaries. *The Journal of Machine Learning Research* **14** 499–566.
- [60] STROBL, C., BOULESTEIX, A.-L., KNEIB, T., AUGUSTIN, T. and ZEILEIS, A. (2008). Conditional variable importance for random forests. *BMC Bioinformatics* **9** 1–11.

- [61] STROBL, C., BOULESTEIX, A.-L., ZEILEIS, A. and HOTHORN, T. (2007). Bias in random forest variable importance measures: Illustrations, sources and a solution. *BMC bioinformatics* **8** 1–21.
- [62] TAN, A. C., NAIMAN, D. Q., XU, L., WINSLOW, R. L. and GEMAN, D. (2005). Simple decision rules for classifying human cancers from gene expression profiles. *Bioinformatics* **21** 3896–3904.
- [63] TIBSHIRANI, R. (1996). Regression shrinkage and selection via the lasso. *Journal of the Royal Statistical Society: Series B (Methodological)* **58** 267–288.
- [64] TONG, Z., CAI, Z., YANG, S. and LI, R. (2022). Model-free conditional feature screening with FDR control. *Journal of the American Statistical Association* 1–13.
- [65] VAN DER LAAN, M. J. (2006). Statistical inference for variable importance. *The International Journal of Biostatistics* **2**.
- [66] WEI, P., LU, Z. and SONG, J. (2015). Variable importance analysis: a comprehensive review. *Reliability Engineering & System Safety* **142** 399–432.
- [67] WILLIAMSON, B. D., GILBERT, P. B., SIMON, N. R. and CARONE, M. (2023). A general framework for inference on algorithm-agnostic variable importance. *Journal of the American Statistical Association* **118** 1645–1658.
- [68] WRIGHT, M. N. and ZIEGLER, A. (2017). ranger: A Fast Implementation of Random Forests for High Dimensional Data in C++ and R. *Journal of Statistical Software* **77** 1–17.
- [69] ZHONG, W., LIU, Y. and ZENG, P. (2023). A model-free variable screening method based on leverage score. *Journal of the American Statistical Association* **118** 135–146.
- [70] ZHU, L.-P., LI, L., LI, R. and ZHU, L.-X. (2011). Model-free feature screening for ultrahigh-dimensional data. *Journal of the American Statistical Association* **106** 1464–1475.